Bioorganic Chemistry 153 (2024) 107884

Contents lists available at ScienceDirect

Bioorganic Chemistry

journal homepage: www.elsevier.com/locate/bioorg

Combining lavendustin C and 5-arylidenethiazolin-4-one-based pharmacophores toward multitarget anticancer hybrids

Shimaa A. Othman [a], Ola F. Abou-Ghadir [a], Varsha Menon [b], Wafaa S. Ramadan [b], Yaser A. Mostafa [a,1], Raafat El-Awady [b], Hajjaj H.M. Abdu-Allah [a,*]

[a] Pharmaceutical Organic Chemistry Department, Faculty of Pharmacy, Assiut University, Assiut 71526, Egypt
[b] Research Institute for Medical and Health Sciences and College of Pharmacy, University of Sharjah, Sharjah 27272, United Arab Emirates

ARTICLE INFO

Keywords:
Anticancer
Lavendustins
5-aminosalicylic
Thiazolin-4-one
Antiproliferative
EGFR
Apoptosis
Debenzylation

ABSTRACT

Lavendustin C, a natural-product derived anticancer lead compound, was modified at its carboxylic group by esterification or amidation (compounds **6**–**10**) and at its amino group by introducing 5-arylidenethiazolin-4-ones (**14a–c** to **17a–c, 18a** and **18b**). Two strategies were used to combine these moieties and to optimize the yield. These new compounds were evaluated for their antiproliferative activities against a panel of nine cancer cell lines. The results clearly show that 5-arylidenethiazolin-4-one moiety contributes substantially to the activity. Also, methyl esters are more potent than amides, while *N*-ethylamides are the most potent among amides. **14b** showed the highest potency against all tested cancer cell lines with IC_{50} 1.4–2.5 μM, while against normal cell line $IC_{50} > 50$ μM. It showed arrest of HeLa cells at G0/G1, S phases and reduction of the percent of cells in G2/M. Moreover, **14b** triggered death of HeLa cancer cells via apoptosis induction. EGFR inhibitory potency of **14b** was found to be comparable to that of erlotinib. Computational docking and *in silico* pharmacokinetic studies were performed and discussed. In conclusion, **14b** might serve as a multitarget lead compound for further development of anticancer agents.

1. Introduction

Cancer is a severe health problem and the leading cause of death worldwide [1,2]. The intricacy of the disease causes and the frequently inadequate specificity of the available medicines have made managing cancers difficult [3]. Adopting pharmacophores as a hybrid molecule that modulates several targets in cancer cells with potential greater therapeutic benefits and a more favorable side effect profile than the effect of selective ligands is a viable strategy to address these issues [4–12]. 4-thiazolinone [13,14] and 5-aminosalicylic acid (5-ASA) [15] are of interest for the hybrid-pharmacophore application [16–20]. Some of 5-ASA-thiazolinone hybrids (Fig. 1) showed potent antiproliferative effects on some types of cancer comparable to doxorubicin with tumor specificity and minimal effects on normal cells [16–20]. Mechanistic investigations of the anticancer activity revealed that this class of compounds potentially act through multitarget mechanism including induction of DNA damage [16,17], cancer cells arrest at the G2/M phase [16,17], induction of apoptosis, and modulation of the metabolomic profile of cancer cells [16].

On the other hand, lavendustin A, and lavendustin B (Fig. 2), are 5-ASA derivatives that were isolated in 1989 from *Streptomyces griseolavendus* as secondary metabolites [21]. Lavendustin A and its synthetic biologically active pharmacophore "lavendustin C" (Fig. 2) are potent inhibitors of epidermal growth factor receptor associated tyrosine kinase (EGFR-TK) [22]. Lavendustin A has a high polarity that decreases its penetration in cellular membranes. Endeavors to improve antiproliferative activity and cell penetration of lavendustin A were started in 1990 [23,24]. These extensive research on lavendustin A structural optimization provided derivatives (Fig. 2) with improved pharmacokinetic properties and efficacy [22–30].

Moreover, some of the derivatives affect other targets besides protein tyrosine kinase (PTKs) inhibition [25,26], including the nonreceptor protein tyrosine kinase (Syk) and tubulin polymerization [27] as well as Aurora kinase [28]. Interestingly, a series of lavendustin C derivatives having *N*-substituted amides (Fig. 2; **V)** revealed potent dual inhibition of COX-2/5-LOX [31]. Research findings indicate that COX-2 and 5-LOX

* Corresponding author.
E-mail address: hajjaj@aun.edu.eg (H.H.M. Abdu-Allah).
[1] Current address: Pharmaceutical Chemistry Department, Faculty of Pharmacy, Badr University in Assiut, Assiut 71511, Egypt.

https://doi.org/10.1016/j.bioorg.2024.107884
Received 19 June 2024; Received in revised form 26 September 2024; Accepted 8 October 2024
Available online 12 October 2024

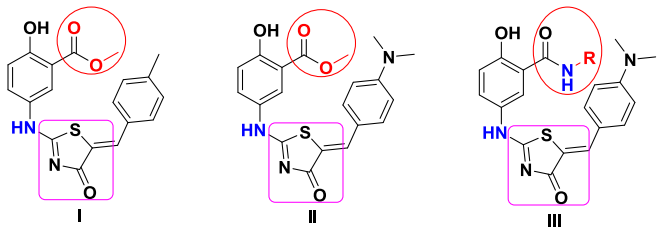

Fig. 1. Some of 5-aminosalicylic thiazolinone hybrids [16–20].

are both co-expressed and up-regulated in numerous malignancies, and the eicosanoids generated by these enzymes play a major role in the growth of these tumors [32–34]. For more effective cancer prevention and therapy, there is a growing interest in the development of innovative COX-2/5-LOX dual inhibitors [32–34]. The above-mentioned information about the potent multitarget anticancer activity of 5-ASA-thiazolinone hybrids, lavendustins A, C and their derivatives inspired us to synthesize lavendustin C thiazolin-4-one hybrids as potential multitarget anticancer agents with better safety profile (Fig. 3). To achieve this goal lavendustin C derivatives modified at the carboxylic group was synthesized (compounds **6**–**10**) and biologically evaluated as antiproliferative then the effect of hybridization with 5-arylidenethiazalin-4-one was investigated. The nature of the substituents at 5-arylidene moiety were selected based on the results of the previous studies [16–20].

2. Results and discussion

2.1. Chemistry

The reactions which have been developed in order to elaborate this library of 14 lavendustin 5-arylidenethiazolin-4-one hybrids are outlined in Schemes 1–3. The synthetic plan involved the synthesis of lavendustin C derivatives (**6**–**10**) having their carboxylic group amidated or esterified for evaluating their antiproliferative activity, then introducing 5-arylidenethiazolin-4-one to get lavendustin thiazolinone hybrids (**14**–**18**). The starting primary amines (**1**–**5**) are known and were synthesized as reported [18,31]. Reductive amination was used for introducing 2,5-dihydroxybenzyl moiety to (**1**–**5**) either by two stepwise reactions (Schiff base formation then reduction using sodium borohydride) as in case of compound **6** or by a modified one pot reaction using sodium cyanoborohydride to obtain the lavendustin C derivatives (**7**–**10**) in a high yield (90 %) and purity to be used in the next step without further purification (Scheme 1). Compounds **6, 9** and **10** are reported [22,31], while compounds **7** and **8** are new and confirmed by appearance of benzylic CH_2 signal at 4.10 ppm in ^{1}H NMR. Our initial plan for the synthesis of hybrids (**14**–**18**) was to introduce thiazolinone moiety through chloroacetylation then cyclization with ammonium thiocyanate (Scheme 1) as we previously reported for 5-aminosalicylamides [18]. Thus, the lavendustin C derivative **10** was chloroacetylated to afford **11** in 85 %. Cyclization of **11** by refluxing with ammonium thiocyanate provided the nitrile derivative **12** at first. Refluxing for longer time (72 h) provided the corresponding thiazolin-4-one **13** in a 50 % yield (Scheme 1). The three intermediates **11**, **12** and **13** are new compounds and were characterized by spectral data. Unexpectedly, Knoevenagel condensation of **13** with different aromatic aldehydes under different reaction conditions [18] failed to give the final 5-arylidene product. More vigorous conditions, heating at higher temperature for longer time, resulted in decomposition of **13** as detected by darkening of the reaction mixture and the appearance of several spots on TLC. Decomposition might be attributed to oxidation of 2,5-dihydroxybenzyl moiety to quinonoid structure.

At this stage, literature was searched for other suitable methods for introducing thiazolinone moiety to a secondary amine under neutral condition and at room temperature to avoid decomposition. An attractive approach was found based on rhodanine chemistry [35,36].

Such approach starts with preparation of rhodanine derivatives (**RD4–6**) on two steps: firstly, acid catalyzed Knoevenagel condensation of rhodanine with 4-methylbenzaldehyde, 4-dimethylaminobenzaldehyde or cinnamaldehyde to give compounds (**RD1–3**) in 95 % yield [37–39]. **RD1–3** were reacted with ethyl bromoacetate to afford S-

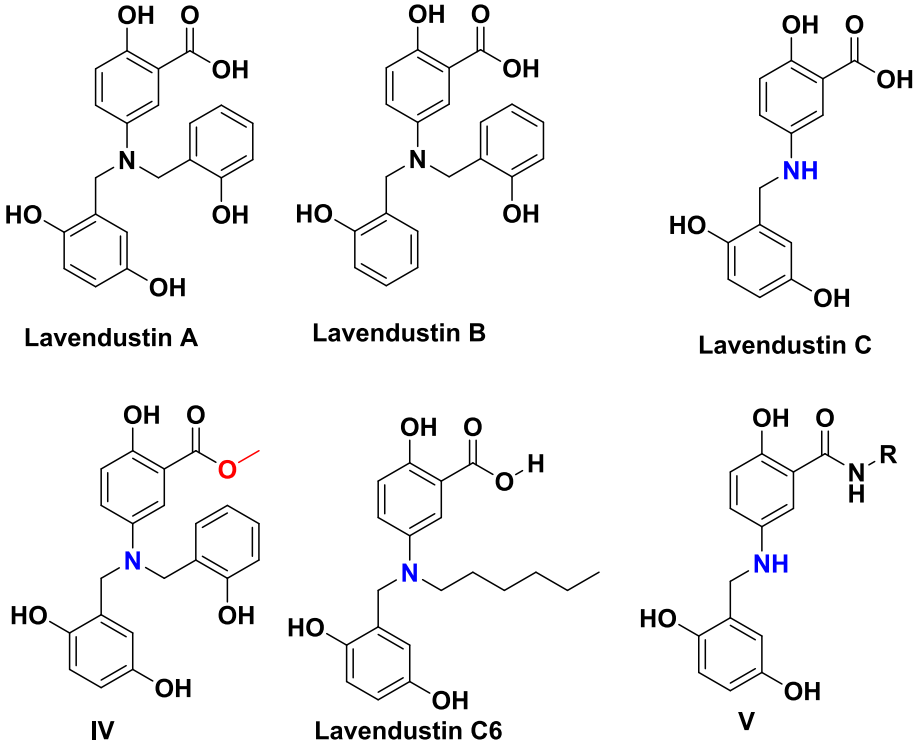

Fig. 2. Structures of some known lavendustin derivatives [22–30].

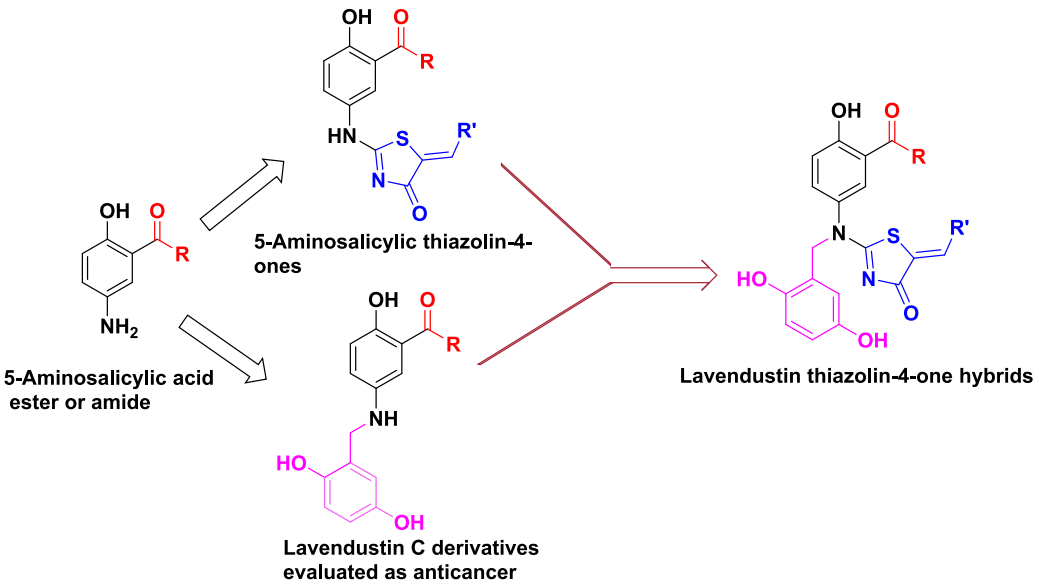

Fig. 3. The designing strategy of the lavendustin thiazolin-4-one hybrids.

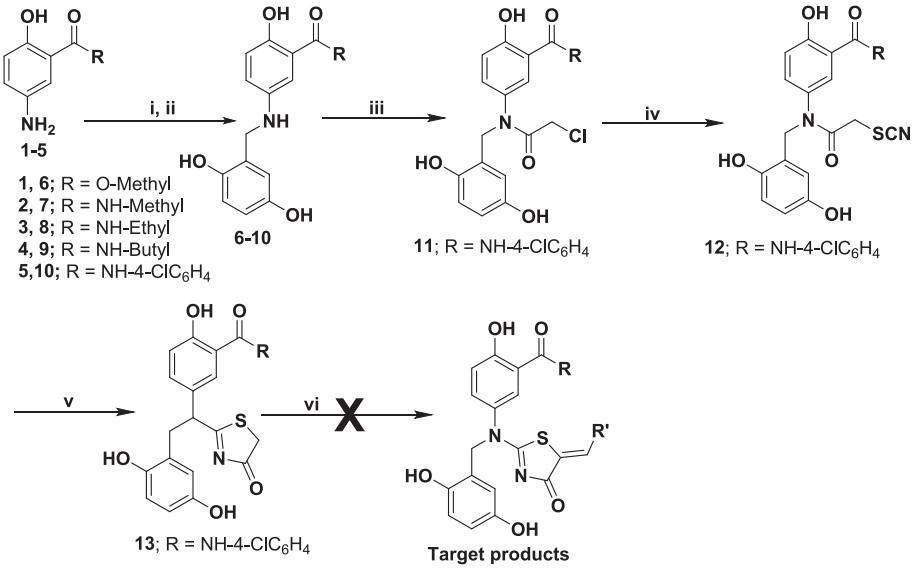

Scheme 1. First strategy for the synthesis of lavendustin C thiazolin-4-one hybrids (**14a–c to 17a–c, 18a** and **18b):** Reagents and conditions:(i) 2,5-dihydroxybenzaldehyde (1 equiv), EtOH, AcOH, rt, 2 h; (ii) $NaCNBH_3$, or $NaBH_4$ (1.5 equiv), EtOH, 0–5 °C, 88–90 %; (iii) Chloroacetyl chloride (1.2 equiv), DMF, rt, 15 min, 85 %; (iv) NH_4SCN, EtOH, reflux, 6 h, 90 % (v) EtOH, reflux, 72 h, 50 %;(v) ArCHO, EtOH, reflux, piperidine.

alkylated rhodanines (**RD4–6**) in a 90–94 % yield (Scheme 2). Rhodanines (**RD4–6**) are new and were characterized by spectral data and used for introducing the thiazolinone moiety to the lavendustin derivatives (**6–10**) (Scheme 2). The reactions between lavendustin C derivatives (**6–10**) and rhodanines (**RD4–6**) were problematic and tried under different conditions for optimization, as listed in Table 1.

The main problem of the reaction was the departure of 2,5-dihydroxybenzyl group (debenzylation) (Scheme 3). The debenzylated side products were isolated and characterized by their physical and spectral data, which were found to be identical to that we previously reported [18,20] for 5-aminosalicylate or 5-aminosalicylamide hybrids with 5-arylidenethiazolin-4-ones (Support. Inform. Fig. 38 and Fig. 39).

We were curious to know the correlation between debenzylation and the introduction of thiazolinone moiety. *O*- and *N*-debenzylation is known under similar conditions [40,41]. The sequence of events for debenzylation and the introduction of thiazolinone moiety can be expected to occur through one of two possible pathways. Debenzylation might have occurred before introducing thiazolinone moiety. Alternatively, the target compounds containing benzyl and thiazolinone moieties might be formed first then undergo debenzylation. This pathway is the logical approach for debenzylation process because the benzyl moiety in this structure becomes more susceptible for oxidation and debenzylation due to the extended conjugation of electron rich system (Scheme 3).

Scheme 3 doesn't really explain a proper chemical reaction mechanism, it is more a scheme with a suggested sequence of events. The key points are that the lone pair of electrons of the exocyclic tertiary *N* are tied up in conjugation with 5-arylidenethiazolin-4-one ring and salicylyl moiety. Also, the presence of two electron donating OH groups make electron-rich aromatic ring facilitating the benzyl leaving.

In support of this assumption is the stability of the cyclized product (compound **13**; Scheme 1) even upon heating for long time without

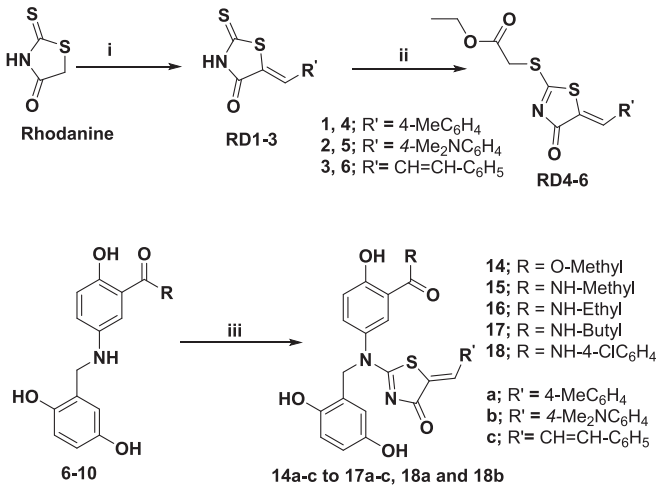

Scheme 2. Second strategy for the synthesis of lavendustin C thiazolin-4-one hybrids (**14a–c** to **17a–c**, **18a** and **18b**): (i) ArCHO, AcOH, AcONa, reflux, 4–6 h, 94–95 %; (ii) Ethyl bromoacetate (1.5 equiv), acetone, TEA, reflux, 4–6 h, 90–94 %; (iii) **RD4–6** (1 equiv), (EtOH: MeCN) (1:1), 50–60 °C, 1–3 days; 10–76 %.

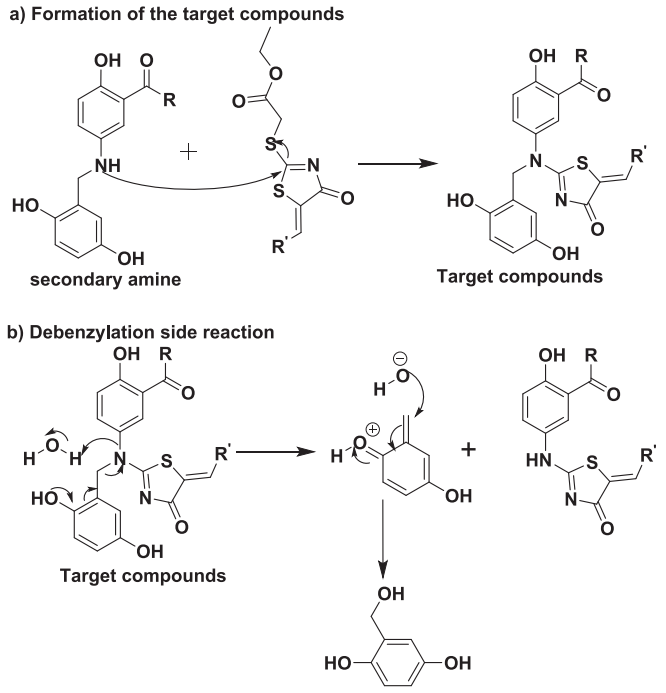

Scheme 3. The proposed sequence of events for debenzylation side reaction.

undergoing debenzylation as discussed in the first strategy. This means that debenzylation occurs for the target tertiary amine with arylidene moiety as it is more conjugated. The side products formed due to debenzylation made it difficult to isolate and purify the targets compounds either by recrystallization or column chromatography. During purification by column chromatography the product was adsorbed on silica gel due to its polarity and elution was very slow even upon using dichloromethane/methanol system. To avoid or minimize debenzylation and purification problems and optimize the reaction yield, several experiments were done (Table 1).

The first condition (entry 1) was tried based on a reported procedure for similar *N*-alkylation [35,36]. However, the debenzylated side product precipitated and obtained as the major product, while the target compound was obtained in very low yield (15 %). Then polar aprotic

Table 1
Optimization of the reaction conditions for the synthesis of the target compounds (**14a–c** to **17a–c**, **18a** and **18b**).

Entry	No. of equiv. of lavendustin C derivative (**6–10**)	No. of equiv. of **RD4-6**	Solvent	Reaction temp/time	Yield%[a]
1	1	1	EtOH	Reflux/2 h	**18a** 15 %
2	1	1	MeCN/ THF	Reflux/4 h	……..[b]
3	1	1–1.5	MeCN	rt/10 days	excess of **RD4–6**
4	1.5	1	MeCN	50–60 °C/6 days	**14b** 50 %
5	1.5	1	MeCN/ EtOH (1:1)	50–60 °C/ 1–3 days	**14–18 (a–c)** Up to 76 %

[a] Product yields achieved after purification.
[b] Purification of compound **14b** was unsuccessful.

solvents such as THF and/or MeCN were used instead of ethanol (entries 2 and 3). Under these conditions poor yields were also obtained. To overcome these limitations, the reaction was tried at 50–60 °C to shorten the reaction time and compound **6** was used in higher ratio (1.5 equivalent) to make the purification easier (entry 4). Fortunately, the target compound **14b** was obtained in 50 % yield but within a very long reaction time. To make the reaction time more reasonable, the last reaction conditions (entry 5), a solvent mixture of EtOH/MeCN was used as a solvent, 1.5 equivalence of lavendustin C derivative and heating at 50–60 °C for 1–3 days, were optimal in reaction of all derivatives (**6–10)** with **RD4** or **RD6.** The products were purified by further double recrystallization to afford (**14a–18a**) and (**14c–17c**) in up to 76 % yield. Fortunately, the debenzylated side product from the reactions of compounds (**6–10)** with **RD5** precipitated from the reaction mixture and was removed by filtration, while the mother liquor was allowed to stand to crystallize the target compound as a single pure product (**14b–18b**). The structures of all final compounds were confirmed by spectral data; IR, NMR (^{1}H and ^{13}C) and elemental analysis. Particularly, the appearance of 4-thiazolinone carbonyl group peak at 1670–1683 cm^{-1} in IR and by ^{1}H NMR by disappearance of NH signal at 5.42 ppm and appearance of different signals of the added arylidene moiety. Interestingly, ^{1}H NMR spectra of the new lavendustin C thiazolin-4-one hybrids (**14a–c to 17a–c, 18a** and **18b**) didn't show doubling of signals which indicates the structural rigidity and the absence of syn/anti arrangement of rotamers that was observed in the case of the corresponding compounds without benzyl group [18,20].

2.2. Biology

2.2.1. Antiproliferative activity

In an effort to improve the therapeutic properties of lavendustins C and A, the structural features from our previous studies that were found to improve the antiproliferative activity of 5-ASA [18,20,31] were introduced to obtain two new series of lavendustin C (**6–10**) and lavendustin A derivatives (**14a–c** to **17a–c**, **18a** and **18b**). The antiproliferative activity of these new derivatives were evaluated to compare the activity between the two series and to study the contribution of 4-thiazolinone moiety to the activity. Therefore, the preliminary screening of the antiproliferative activity of all target compounds **6–10**, **14a–c** to **17a–c**, **18a** and **18b** was firstly evaluated against the three most sensitive cancer cell lines [18,20] (MCF-7, Jurkat and U937) at 10 μM concentration compared to doxorubicin as the reference drug. The screening results showed that most of the tested tertiary compounds (**14a–c** to **17a–c**, **18a** and **18b**) have higher antiproliferative activity against the Jurkat (T cell) and U937 (monocytic) cell lines. This observation refers to the significant contribution of thiazolinone moiety to the

activity. Compounds without this moiety (**6**–**10**) showed activity only against Jurkat leukemia cell line (see Figs. S1–S17). The improved activity of the new hybrids (**14a–c, 15a, 16b** and **17a–c**) could be attributed, in part, to enhanced lipophilicity caused by 5-arylidenethiazolinone moiety according to their calculated cLogP values 3.85–4.66 (*c.f. N*-benzylated derivatives cLogP = 1.96–3.37), as listed in Table 6. Compounds with the highest antiproliferative activities (**14a–14c, 15b, 16b** and **17a–c)** were subjected to a full concentration–response analysis to determine their IC_{50} (Table 2). Generally, ester and amides hybrids caused significant inhibition to lymphoma cells (IC_{50} = 2.51–50 μM). Remarkably, the methyl esters (**14a–c**) showed higher potency than their amidic analogues (**15**–**16a–c**); compound **14b** was about 3.5-fold more potent than **16b** against Jurkat leukemia cell line (IC_{50} = 1.44 & 4.93 μM; respectively) (Table 2). Moreover, the chain length of the amidic *N*-substituent was found to significantly affect the activity; *N*-ethyl derivative **16b** was 2-fold more potent than *N*-butyl derivative **17b** as antiproliferative agent against Jurkat leukemia and lymphoma cell lines (IC_{50} **16b**; 4.93 μM, 11.12 μM, **17b**; 8.06 μM, 23.07 μM; respectively) (Table 2), while the *N*-methyl derivative **15b** showed weaker activity. As shown in Table 2, all tested compounds showed no significant cytotoxicity towards normal fibroblast cells F180 (IC_{50} > 50 μM) indicating their high safety profile (*c.f.* doxorubicin).

Furthermore, the most active compounds **14a–c** were evaluated against six cancer cell lines from different histological backgrounds to evaluate their antiproliferative spectrum (Table 3). Interestingly, **14a** and **14b** revealed the highest potency against all tested cancer cell lines. Particularly**, 14b** is 2–3-fold more potent than **14a** against most tested cell lines with IC_{50} values (1.44–5.58 μM) (Table 3). However, they showed comparable potency against lymphoma cell line U937 (IC_{50} = 2.51, 2.97 μM; respectively).

Regarding the glioblastoma U87 cell line, the new lavendustin derivatives enhanced the antiproliferative activity, particularly, compound **14a** and **14b** showed good activity with IC_{50} values of 8.95 and 5.58 μM; respectively. Interestingly, compound **14b** showed good activity against the resistant lung adenocarcinoma cell line (A549) with IC_{50} = 4.13 μM and compound **14a** came in the second (IC_{50} = 8.03 μM) (Table 3). Accordingly, compound **14b** showed the highest potency against 7 cancer cell lines and is non-cytotoxic to normal cell line. Therefore, it was used to explore the possible molecular mechanism of action as follow:

2.2.2. Cell cycle analysis

To get a deeper insight into the mechanism of antiproliferative activity of the new compounds, the effect of compound **14b** on the cell cycle progression of HeLa cells was investigated. Treatment of HeLa cells with **14b** showed arrest of cells at G0/G1 and S phases and reduction of the percent of cells in G2/M in treated cells compared to control cells. For **14b**-treated HeLa cells the percent of cells at the different phases of the cell cycle were 55.15 % (G0/G1), 43.19 % (S), 1.66 % (G2/M) compared to 46.38 % (G0/G1), 38.11 % (S), and 15.51 % (G2/M) in the control HeLa cells (Fig. 4).

Table 2
IC_{50} of new lavendustin thiazolinone hybrids **14a–c,** 15**a, 16b, 17a–c** and **DOX** against MCF-7, Jurkat, U937 and normal fibroblast cell lines.

Compd. No.	IC_{50} (μM)			
	MCF-7	Jurkat	U937	F180
14a	6.41 ± 0.12	3.50 ± 0.12	2.97 ± 0.12	>50
14b	**3.26 ± 0.10**	**1.44 ± 0.12**	**2.51 ± 0.13**	**>50**
14c	>50	6.98 ± 0.11	8.39 ± 0.11	>50
15a	>50	>50	20.78 ± 0.09	>50
16b	18.19 ± 0.09	4.93 ± 0.11	11.12 ± 0.10	>50
17a	>50	>50	8.61 ± 0.11	>50
17b	>50	8.06 ± 0.10	23.04 ± 0.08	>50
17c	>50	>50	8.78 ± 0.11	>50
DOX	0.13 ± 0.11	0.55 ± 0.12	0.31 ± 0.09	0.62 ± 0.12

Represented data means ± SEM of 3 independent experiments; ND: not determined.

Table 3
IC_{50} of **14a–c** and DOX against 6 cancer cell lines.

Compd. No.	IC_{50} (μM)					
	MDA MB-231	A549	HCT-116	U87	U373	HeLa
14a	6.53 ± 0.12	8.05 ± 0.11	6.32 ± 0.11	8.95 ± 0.12	15.45 ± 0.09	6.84 ± 0.11
14b	ND	**4.13 ± 0.10**	**2.11 ± 0.12**	**5.58 ± 0.11**	>50	**2.04 ± 0.12**
14c	ND	>50	>50	>50	>50	>50
DOX	0.72 ± 0.10	0.27 ± 0.11	0.17 ± 0.11	0.25 ± 0.10	0.75 ± 0.09	0.21 ± 0.12

Represented data means ± SEM of 3 independent experiments; ND: not determined.

2.2.3. Apoptosis assay

Apoptosis is a common death pathway in cancer cells after treatment with anti-cancer agents. Therefore, the induction of apoptosis in HeLa cells after incubation with compound **14b** was investigated. The results showed a significant induction of early and late apoptosis in a high percentage (33 %) of **14b**-treated HeLa cells. Whereas only 6.41 % of the treated cells showed necrosis (Fig. 5).

2.2.4. EGFR inhibition

Several solid tumors including colon, breast, ovarian, lung and prostate cancer have been reported previously to overexpress EGFR [42]. Therefore, EGFR is recognized as a conventional target for cancer therapy [27]. Moreover, previous studies have attributed the anticancer activity of lavendustin derivatives to EGFR inhibition [22,25–27]. Thus, the effects of compounds **14a, 14b** and **16b** on EGFR were studied and revealed IC_{50} values in the low micromolar range (IC_{50} = 0.88, 0.19, & 1.6 μM; respectively; *c.f* erlotinib, IC_{50} = 0.11 μM) (Table 4). That means **14b** is the most potent inhibitor of EGFR and is comparable in potency to erlotinib.

2.3. Molecular docking study

In the light of the results obtained against all tested cancer lines and against EGFR enzyme, *in silico* docking simulations were performed for the most potent antiproliferative derivatives **14a, 14b** and **16b** in order to study their molecular interactions with amino acid residues lining EGFR active site (Table 5). Concerning docking score analysis, compounds **14a** and **14b** exhibited the highest negative values (−8.14 Kcal/mol and −8.45 Kcal/mol; respectively) which are compatible with their *in vitro* EGFR inhibition effects. Visualization of the ligand protein complexes revealed that the introduction of 5-arylidenethiazolin-4-one rings to the lavendustin C derivative **6** to afford tertiary lavendustin derivatives **14a–c**, considerably enhances their binding mode and hydrophobic interactions with the surrounding amino acid residues. This is due to its increased Van der Waals volume within the active site. Compound **6** showed a much lower negative energy score (−5.58 Kcal/mol) and missing interaction with the key amino acid Met769 (Fig. 6). On the other hand, compounds **14a** and **14b,** (Fig. 6; C–F) bind comfortably inside the large binding pocket. Compound **14a** interacted with the active site of EGFR via strong hydrogen bonding of oxygen of thiazolinone moiety with the key amino acid Met769 (3.07 Å) compared to erlotinib (3.15 Å). In addition to the accepted H-bonding of thiazolinone moiety to the key amino acid Met769 (3.14 Å), compound **14b** forms another weak H-bonding interaction with Glu738 (3.41 Å) through the phenolic OH of the benzyl ring. It is known that hydrogen bonding stabilizes the molecule within the active site of target protein, hence compound **14b** has better interaction profile compared to its congener **14a** and that can explain its higher antiproliferative activity. Regarding

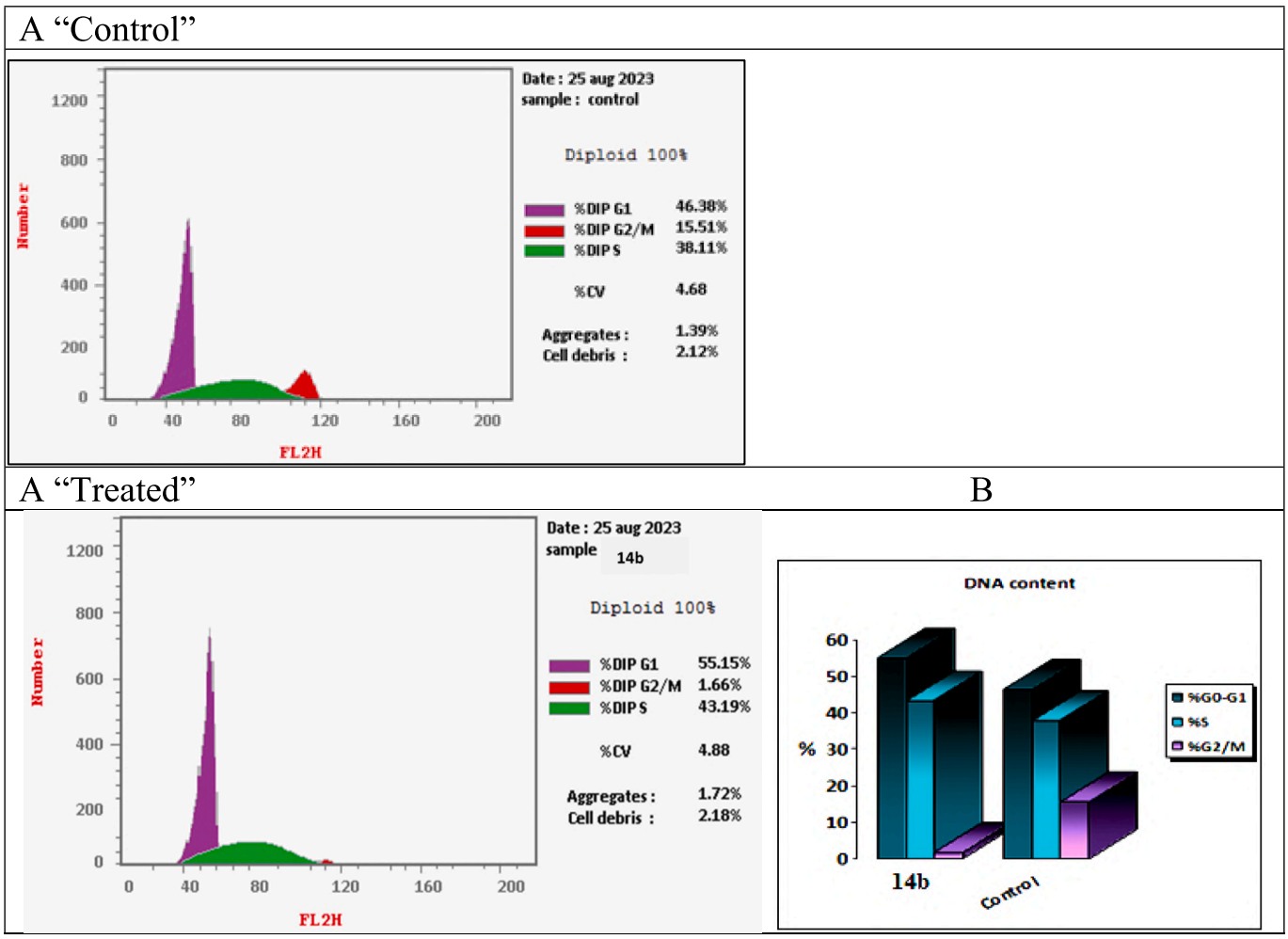

Fig. 4. Cell cycle arrest induced by **14b**. **(A)** Analysis by quantification of DNA content with flow cytometry in control (upper) and **14b**-treated (lower) HeLa cell line. **(B)** Histogram displays the percentage of cell cycle distribution after treatment with **14b**.

the effects of derivatization on the carboxylic acid group, the ester derivatives showed higher potency than the amide derivatives as antiproliferative activity and EGFR inhibitory activity. The lower EGFR inhibitory activity of amide derivatives could be attributed to the missing interaction with the key amino acid Met769 compared with that of erlotinib. Alternatively, the ligand stabilizes its complex by donating a H-bond to Asp831 via the phenolic OH in benzyl moiety with (3.17 Å) and two pi-H interaction with Phe699 (4.41 Å) through the ethyl side chain and Val702 (4.20 Å) through the thiazolin-4-one moiety in case of compound **16b** (Fig. 7).

2.4. *In silico studies*

The most potent antiproliferative lavendustin hybrids **6**, **8**–**10**, **14a–c, 15a, 16b,** and **17a–c** were examined for their physicochemical properties. The *in silico* pharmacokinetic data of lavendustin derivatives (Table 6) showed that all the studied compounds have the appropriate drug-like properties as they obey Lipinski's rule of five. These results reveal that the enhancement of the antiproliferative activity might be attributed to the significant increase in lipophilicity.

3. Conclusions

New lavendustin derivatives were synthesized through dual modification of its carboxylic and amino groups. Esterification or amidation of the carboxylic group provided compounds (**6**–**10**). 5-Arylidenethiazolin-4-ones were introduced to **6**–**10** through reaction with the appropriate rhodanine derivatives to afford compounds (**14a–c** to **17a–c**, **18a** and **18b)** in yield up to 76 % after optimization efforts. These compounds were evaluated for their antiproliferative activity against a panel of nine cancer cell lines. The results showed that the new tertiary lavendustin derivatives (**14a–c** to **17a–c**, **18a** and **18b**) showed higher potency than the corresponding secondary lavendustin C derivatives (**6**–**10**). In addition, these derivatives showed a broad range of antiproliferative activity against all tested cancer cell lines in contrast to compounds (**6**–**10**) that showed a good activity only against Jurkat leukemia. Compound **14b** was the most potent among this series against all cancer cell lines particularly against Jurkat leukemia and lymphoma U937 with IC_{50} 1.44, 2 μM; respectively. The most active compounds **14a**, **14b** and **16b** were evaluated for EGFR inhibitory potency. Compound **14b** was the most potent and its IC_{50} is comparable to the standard drug (erlotinib). Moreover**, 14b** showed arrest of cells at G0/G1 and S phases and reduction of the percent of cells in G2/M in cell cycle assay. The results of apoptosis induction assay revealed that **14b** strongly induced apoptosis in HeLa cells. Thus, **14b** is a promising multitarget lead compound for anticancer drug development. Further scientific efforts are still in demand to seek more adequate and flexible synthetic methodologies of novel 5-aminosalicylate based scaffolds. Taking into consideration the referred biological outcome due to hybridization with 5-arylidenethiazolin-4-ones, the interest is particularly focused on the chemical transformations related to improving solubility and efficacy for *in vivo* studies.

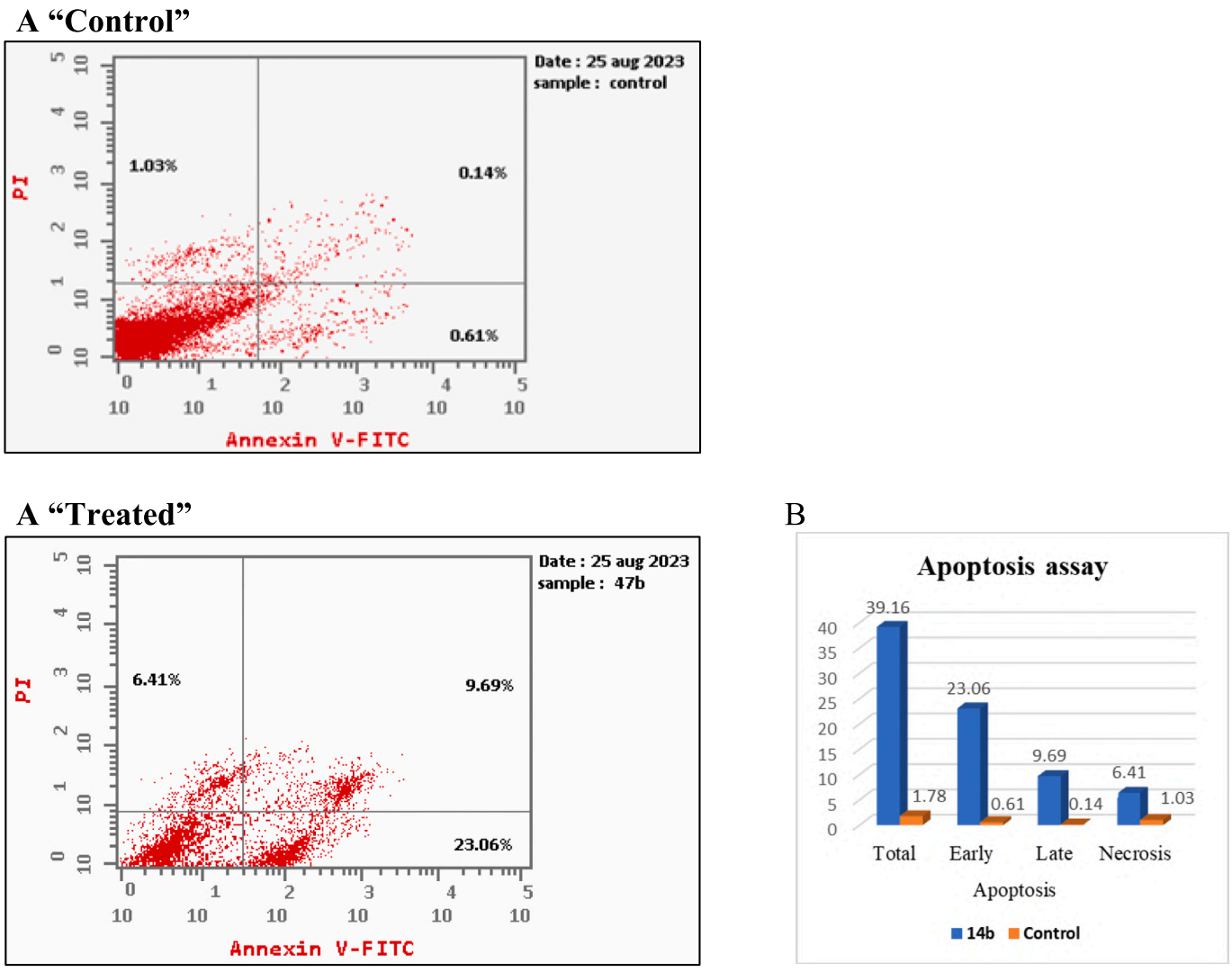

Fig. 5. Analysis of apoptosis induction in HeLa cells treated with compound **14b**. (A) Flow cytometric presentation of population of cells showing early/late manifestations of apoptosis with the indicated concentration of **14b** (IC_{50}: 2.04 μM); The HeLa cells were 'stained with Annexin V/FITC and propidium iodide. Q1: Necrosis, Q2: late apoptosis, Q3: viability, Q4: early apoptosis. (B) Quantitative presentation of percent of cells showing early, late apoptosis or necrosis compared to control cells; x-axis represents compound number and apoptosis phase, while y-axis represents % of the apoptotic cells.

Table 4
EGFR inhibitory potencies of **14a, 14b, 16b** and **erlotinib**.

Compd. No	IC_{50} (μM)			
	14a	**14b**	**16b**	**Erlotinib**
EGFR	0.88 ± 0.04	0.19 ± 0.009	1.6 ± 0.08	0.11 ± 0.005

Table 5
Docking score (S) of test compounds within the active site of EGFR.

Compd. No.	S (Kcal/mol)	Binding interactions		
		Bond Type	Bond Length (Å)	a. a. residue
6	−5.58	H-donor	3.21 Å	Glu738
14a	−8.14	H-acceptor	3.07 Å	Met769
14b	−8.45	H-acceptor	3.14 Å	Met769
		H-donor	3.41 Å	Glu738
16b	−6.93	H-donor	3.17 Å	Asp831
		pi-H	4.41 Å	Phe699
		pi-H	4.20 Å	Val702
Erlotinib	−7.3	H-acceptor	2.70 Å	Met769
		H-donor	3.15 Å	Gln767

4. Experimental

4.1. Chemistry

4.1.1. General

All reagents and solvents were obtained from commercial suppliers and used without further purification except THF which had been dried through reflux with sodium metal and benzophenone followed by distillation over molecular sieves 4A. Melting points were determined on an electrothermal melting point apparatus (Stuart Scientific, model SMP3, England, UK), and were uncorrected. Aluminum-packed thin layer chromatography (TLC) plates (Kieselgel 0.25 mm, 60G F254, Merck, Germany) were used for reactions monitoring. UV light was used for detection at 254 nm and 365 nm wavelengths (Spectroline, model CM-10, USA). IR spectra (KBr discs) were recorded on thermo scientific nicolet IS10 FT IR spectrometer (thermo Fischer scientific, USA) at Faculty of science, Assiut University, Assiut, Egypt. ^{1}H NMR spectra of the intermediates were recorded on a Varian EM-360 L NMR spectrometer (60 MHz, Varian, CA, USA) at Faculty of pharmacy, Assiut University, Assiut, Egypt. Key intermediates and final compounds ^{1}H NMR and ^{13}C NMR were scanned on Avance-III, High performance FT-NMR spectrum, Bruker biospin international AG-Switzerland at 400

Table 6
Physicochemical properties (Lipinski parameters) of compounds **6**, **8**–**10**, **14a–c, 15a, 16b** and **17a–c**.

Compd. No.	M. Wt.	cLogP	Rotatable Bonds	HBD	HBA	TPSA	Violations
6	289.28	1.96	5	4	5	99.02 Å^2	0 violation
8	302.33	1.87	6	5	4	101.82 Å^2	0 violation
9	330.38	2.49	8	5	4	101.82 Å^2	0 violation
10	384.81	3.37	6	5	4	101.82 Å^2	0 violation
14a	490.53	3.85	7	3	7	144.96 Å^2	0 violation
14b	519.57	3.56	8	3	7	148.20 Å^2	1 violation
14c	502.54	4.01	8	3	7	144.96 Å^2	1 violation
15a	489.54	3.46	7	4	6	147.76 Å^2	0 violation
16b	532.61	3.58	9	4	6	151.00 Å^2	1 violation
17a	531.62	4.53	10	4	6	147.76 Å^2	1 violation
17b	560.66	4.21	11	4	6	151.00 Å^2	1 violation
17c	543.63	4.66	11	4	6	147.76 Å^2	1 violation

MHz at faculty of science, Zagazig University, Egypt. Chemical shifts are expressed in δ-values (ppm) relative to TMS as an internal standard, using DMSO-d_6 or $CDCl_3$ as solvents. Sometimes the chemical shifts of the remaining protons of the deuterated solvent served as internal standards. For DMSO-d_6; δ ^{1}H: 2.49 ppm, ^{13}C: 39.7 ppm, while for $CDCl_3$; δ ^{1}H: 7.26 ppm, ^{13}C: 77.16 ppm. Coupling constants (*J*) are reported in Hertz (Hz). Elemental microanalyses were performed on elemental analyzer model flash 2000 thermo fisher at the regional center for mycology and biotechnology (RCMB), faculty of science, Al-Azhar University, Nasr city, Cairo, Egypt for all new compounds.

*4.1.2. General method for the synthesis of 2-hydroxy-5-(N-(2,5-dihydroxybenzyl)amino)-N-(un/substituted)benzamides **(7–10)***

To a stirred solution of the appropriate amine **(2** or **3–5)** (2 mmol, 1 equiv.) in absolute ethanol (10 mL), 2,5-diydroxybenzaldehyde (0.28 g, 2 mmol, 1 equiv.), and 2–3 drops of glacial acetic acid were added. The mixture was stirred at room temperature for 2 h. After the reaction was almost completed, it was cooled to 0–5 °C and $NaCNBH_3$ (0.156 g, 2.5 mmol, 1.25 equiv.) was added in portions with pH adjustment at 4–6 using glacial acetic acid. The resulting mixture was stirred in ice bath for 5–30 min, the solvent was evaporated, brine 15 mL was added to the reaction mixture and the solution was then extracted by ethyl acetate (4 × 30 mL). The organic layer was washed with brine, dried over Na_2SO_4, and evaporated to obtain compound **7**–**10**. Compounds **6, 9** and **10** are reported [22,31], while **7** and **8** that are new and characterized by IR, ^{1}H NMR spectral data.

*4.1.2.1. 2-Hydroxy-5-(N-(2,5-dihydroxybenzyl)amino)-N-methylbenzamide **(7)**.* White powder; yield: 90 %; m.p. 168–170 °C; IR (KBr, ύ cm^{-1}): 3386, 3276, 3026, 2885, 2840, 1645, 1595, 1551, 1492, 1334, 1232, 1195, 996, 869, 862, 779, 696, 542; ^{1}H NMR (400 MHz, DMSO-d_6) $\delta = 11.63$ (s, 1H; OH), 8.78 (brs, 1H; OH), 8.63 (q, $J = 4.8$ Hz, 1H; NHCH$_3$), 8.57 (brs, 1H; OH), 7.01 (d, $J = 2.8$ Hz, 1H; ArH-6), 6.77, 6.75 (dd, $J = 8.8$, 2.8 Hz, 1H; ArH-4), 6.67 (d, $J = 8.8$ Hz, 1H; ArH-3), 6.64 (d, $J = 2.7$ Hz, 1H; ArH-6′), 6.61 (d, $J = 8.6$ Hz, 1H; ArH-3′), 6.45, 6.43 (dd, $J = 8.6$, 2.7 Hz, 1H; ArH-4′), 5.42 (brs, 1H; NHCH$_2$ Benzyl), 4.13–4.09 (m, 2H; NHCH$_2$ Benzyl), 2.78 (d, $J = 4.4$ Hz, 3H; NHCH$_3$ Methyl).

*4.1.2.2. N-Ethyl-2-hydroxy-5-(N-(2,5-dihydroxybenzyl)amino)benzamide **(8)**.* White powder; yield: 92 %; m.p. 145–147 °C; IR (KBr, ύ cm^{-1}): 3385, 3316, 3069, 3042, 2974, 2937, 2849, 1649, 1595, 1552, 1505, 1475, 1386, 1239, 1197, 1048, 993, 897, 824, 773, 722, 576; ^{1}H NMR (60 MHz, DMSO-d_6) $\delta = 8.65$ (brs, 2H; OH, NH), 7.30–6.50 (m, 6H; ArH), 5.33 (brs, 1H; NHCH$_2$ benzyl), 4.20 (s, 2H; NHCH$_2$ benzyl), 3.40–3.15 (m, 2H; NHCH$_2$ Ethyl), 1.23 (t, $J = 5.4$ Hz, 3H; CH$_2$CH$_3$ Ethyl).

*4.1.3. Synthesis of 5-(2-chloro-N-(2,5-dihydroxybenzyl)acetamido)-N-(4-chlorophenyl)-2-hydroxybenzamide **(11)***

Chloroacetyl chloride (3.11 mmol, 1.2 equiv) dropwise with stirring to a cooled solution of (**10**) (1 g, 2.6 mmol) in dry DMF (10 mL). The mixture was stirred for 15 min. Cold water 15 mL was added and stirred for 5 min, and the precipitate formed was filtered, washed with hydrochloric acid (2 %), and water and dried to afford compound (**11**).

White powder; yield: 85 %; m.p. 240–242 °C; IR (KBr, ύ cm^{-1}): 3339, 3069, 2953, 1655, 1607, 1543, 1497, 1208, 863, 828, 791, 746, 695; ^{1}H NMR (400 MHz, DMSO-d_6) $\delta = 11.82$ (s, 1H; OH), 10.41 (s, 1H; NH-4-ClC$_6$H$_4$), 8.70 (brs, 2H; OH), 7.85 (d, $J = 2.6$ Hz, 1H; ArH-6), 7.73 (d, $J = 8.9$ Hz, 2H; ArH-3′,5′ 4-ClC$_6$H$_4$), 7.44 (d, $J = 8.9$ Hz, 2H; ArH-2′,6′ 4-ClC$_6$H$_4$), 7.27, 7.25 (dd, $J = 8.7$, 2.6 Hz, 1H; ArH-4), 6.96 (d, $J = 8.7$ Hz, 1H; ArH-3), 6.60 (d, $J = 2.9$ Hz, 1H; ArH-6″ benzyl), 6.55 (d, $J = 8.6$ Hz, 1H; ArH-3″ benzyl), 6.47, 6.45 (dd, $J = 8.6$, 2.9 Hz, 1H; ArH-4″ benzyl), 4.74 (s 2H; CH$_2$ Benzyl), 4.14 (s, 2H; CH$_2$Cl).

*4.1.4. Synthesis of N-(4-chlorophenyl)-2-hydroxy-5-(N-(2,5-dihydroxybenzyl)-2-thiocyanatoacetamido)benzamide **(12)***

A solution of (**11**) (1 g, 2.17 mmol) and NH_4SCN (0.25 g, 3.25 mmol) in 20 ml EtOH was refluxed for 6 h and then allowed to cool. The obtained precipitate was filtered, washed with water and dried to afford compound (**12**).

White powder; yield: 90 %; m.p. 212–214 °C; IR (KBr, ύ cm^{-1}): 3385, 3001, 2947, 2160, 1652, 1607, 1541, 1497, 1199, 822, 758, 700; ^{1}H NMR (400 MHz, DMSO-d_6) $\delta = 10.74$ (s, 1H; NH-4-ClC$_6$H$_4$), 8.70 (brs, 2H; OH benzyl), 8.05 (s, 1H; ArH-6), 7.80 (d, $J = 8.9$ Hz, 2H; ArH-3′,5′ 4-ClC$_6$H$_4$), 7.47–7.39 (m, 2H; ArH-2′,6′ 4-ClC$_6$H$_4$), 7.28, 7.26 (dd, $J = 8.7$, 2.6 Hz, 1H; ArH-4), 7.03 (d, $J = 8.8$ Hz, 1H; ArH-3), 6.66 (d, $J = 2.9$ Hz, 1H; ArH-6″ Benzyl), 6.58 (d, $J = 8.6$ Hz, 1H; ArH-3″ Benzyl), 6.47, 6.45 (dd, $J = 8.6$, 2.9 Hz, 1H; ArH-4″ Benzyl), 4.74 (s 2H; CH$_2$ Benzyl), 4.20 (s, 2H; CH$_2$CN).

*4.1.5. Synthesis of N-(4-Chlorophenyl)-2-hydroxy-5-(N-(2,5-dihydroxybenzyl)-N-(4-oxo-4,5-dihydrothiazol −2-yl)amino)benzamide **(13)***

A solution of (**12**) (0.5 g, 1.09 mmol) in 15 ml EtOH was refluxed for 72 h and then allowed to stand overnight. The mixture was then evaporated under vacuum, and the obtained residue was washed with water, dried, and finally recrystallized from aqueous EtOH to afford the compound (**13**). Beige powder; yield: 50 %; m.p. 246–248 °C; IR (KBr, ύ cm^{-1}): 3327, 2903, 1632, 1605, 1541, 1494, 1455, 820, 743; ^{1}H NMR (400 MHz, DMSO-d_6) $\delta = 10.51$ (s, 1H; NH-4-ClC$_6$H$_4$), 8.66 (brs, 2H; OH benzyl), 7.79 (s, 1H; ArH-6), 7.79 (d, $J = 8.9$ Hz, 2H; ArH-3′,5′ 4-ClC$_6$H$_4$), 7.41 (d, $J = 8.9$ Hz, 2H; ArH-2′,6′ 4-ClC$_6$H$_4$), 7.17 (d, $J = 8.9$ Hz, 1H; ArH-4), 6.90 (d, $J = 8.8$ Hz, 1H; ArH-3), 6.53 (d, $J = 8.6$ Hz, 1H; ArH-3″,6″ Benzyl), 6.44 (d, $J = 8.6$ Hz, 1H; ArH-4″ Benzyl), 4.69 (s 2H; CH$_2$ Benzyl), 3.55 (s, 2H; CH$_2$ thiazole).

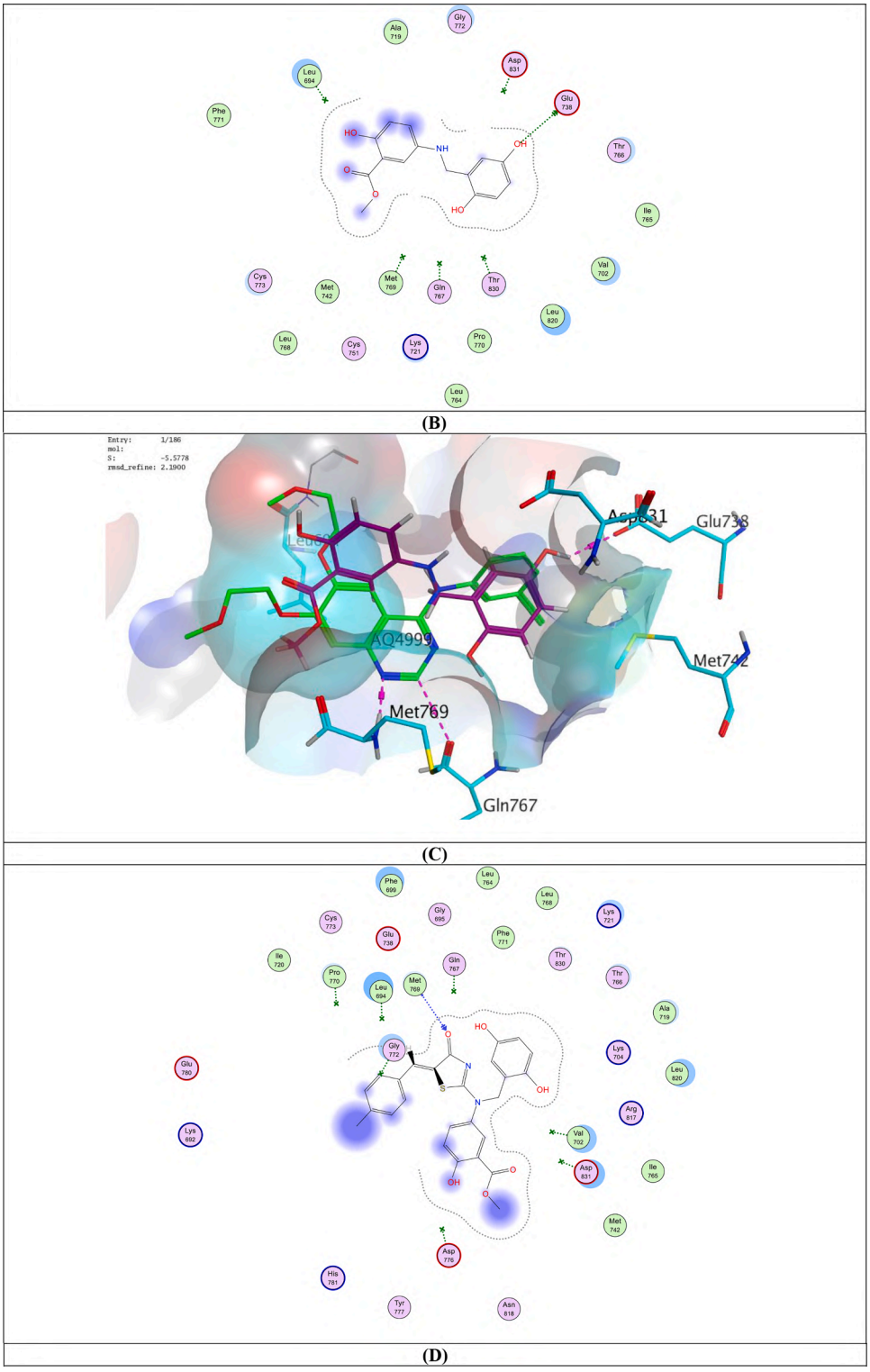

Fig. 6. Docking representation models within the binding site of EGFR; **A** Ligand Interactions Profile of compound 6; **B**: 3D-docked models of compound **6** (purple) overlapped with erlotinib (green); **C**: 2D-docked model of compound **14a**; **D**: 3D-docked models of compound **14a** (purple) overlapped with erlotinib (green); **E**: 2D-docked model of compound **14b**; **F**: 3D-docked models of compound **14b** (pink) overlapped with erlotinib (green). (For interpretation of the references to colour in this figure legend, the reader is referred to the web version of this article.)

*4.1.6. General method for synthesis of ethyl (Z)-2-((5-(substituted)-4-oxo-4,5-dihydrothiazol-2-yl)thio)acetate **(RD4–6)***

To a solution of (**RD1, RD2** or **RD3**) (4.25 mmol, 1 equiv.), in a dried acetone 15 mL, TEA (0.7 mL, 5 mmol, 1.17 equiv.) was added. The reaction mixture was stirred for 5 min, then, ethyl bromoacetate (0.7 mL, 6.37 mmol, 1.5 equiv.) was added and the reaction mixture was refluxed for 4–6 h. The reaction then was cooled, and the precipitate was filtered, washed with fresh acetone, and recrystallized from aqueous

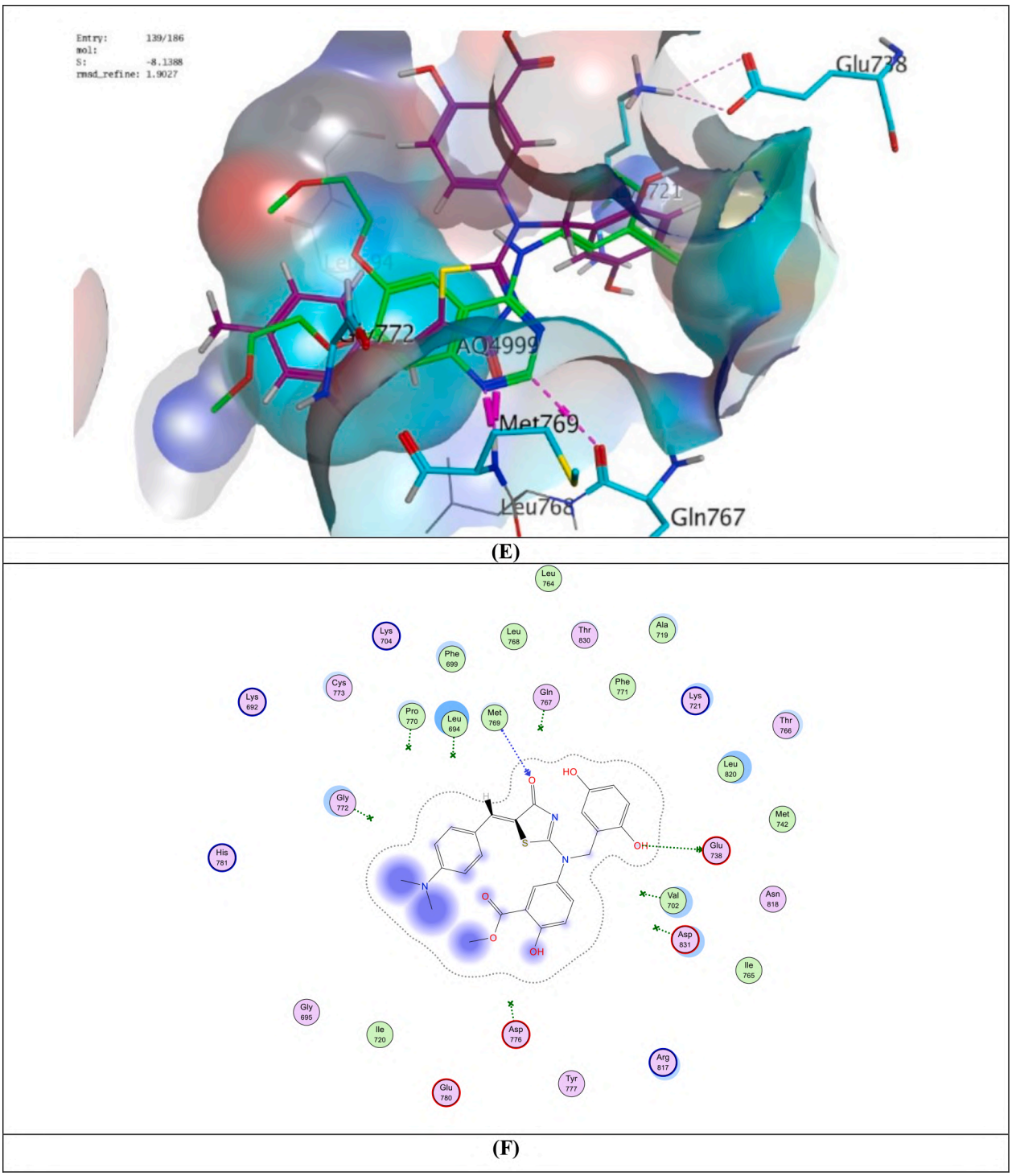

Fig. 6. (*continued*).

ethanol to afford new target alkylating agents **RD4–6**. Compound **RD6** was reported [43] but without sufficient characterization data.

*4.1.6.1. Ethyl (Z)-2-((5-(4-methylbenzylidenyl)-4-oxo-4,5-dihydrothiazol-2-yl)thio)acetate **(RD4)**.* Orange crystals; yield: 94 %; m.p. 163–164 °C; IR (KBr, ύ cm^{-1}): 3000, 2984, 2934, 1743, 1699, 1596, 1476, 1299, 1180, 1143, 996, 812, 695; ^{1}H NMR (400 MHz, $CDCl_3$) $\delta = 7.85$ (d, $J =$ 3.4 Hz, 1H; =CH), 7.41, 7.39 (dd, $J = 8.2$, 3.4 Hz, 2H, ArH-2,6), 7.27, 7.26 (dd, $J = 8.2$, 3.4 Hz, 2H, ArH-3,5), 4.28– 4.21 (m, 4H; $2CH_2$), 2.39 (d, $J = 3.3$ Hz, 3H, 4-MeC_6H_4), 1.30 (td, $J = 7.2$, 3.2 Hz, 3H CH_2CH_3).

*4.1.6.2. Ethyl (Z)-2-((5-(4-(dimethylamino)benzylidenyl)-4-oxo-4,5-dihydrothiazol-2-yl)thio) acetate **(RD5)**.* Red crystals; yield: 90 %; m.p. 155–157 °C; IR (KBr, ύ cm^{-1}): 3050, 2975, 2936, 1748, 1683, 1612, 1574, 1474, 1375, 1180, 1154, 1135, 978, 811, 699; ^{1}H NMR (60 MHz, $CDCl_3$) $\delta = 7.85$ (s, 1H; =CH), 7.50 (d, $J = 8.0$ Hz, 2H; ArH-2,6), 6.80 (d, $J = 8.0$ Hz, 2H; ArH-3,5), 4.55–4.15 (m, 4H; $2CH_2$), 3.20 (s, 6H; $(CH_3)_2$ 4-$Me_2NC_6H_4$), 1.50 (t, $J = 6.0$ Hz, 3H; CH_3).

*4.1.6.3. Ethyl (Z)-2-((4-oxo-5-((E)-3-phenylallylidenyl)-4,5-dihydrothiazol-2-yl)thio)acetate **(RD6)**.* Orange crystals; yield: 90 %; m.p. 125–127 °C; IR

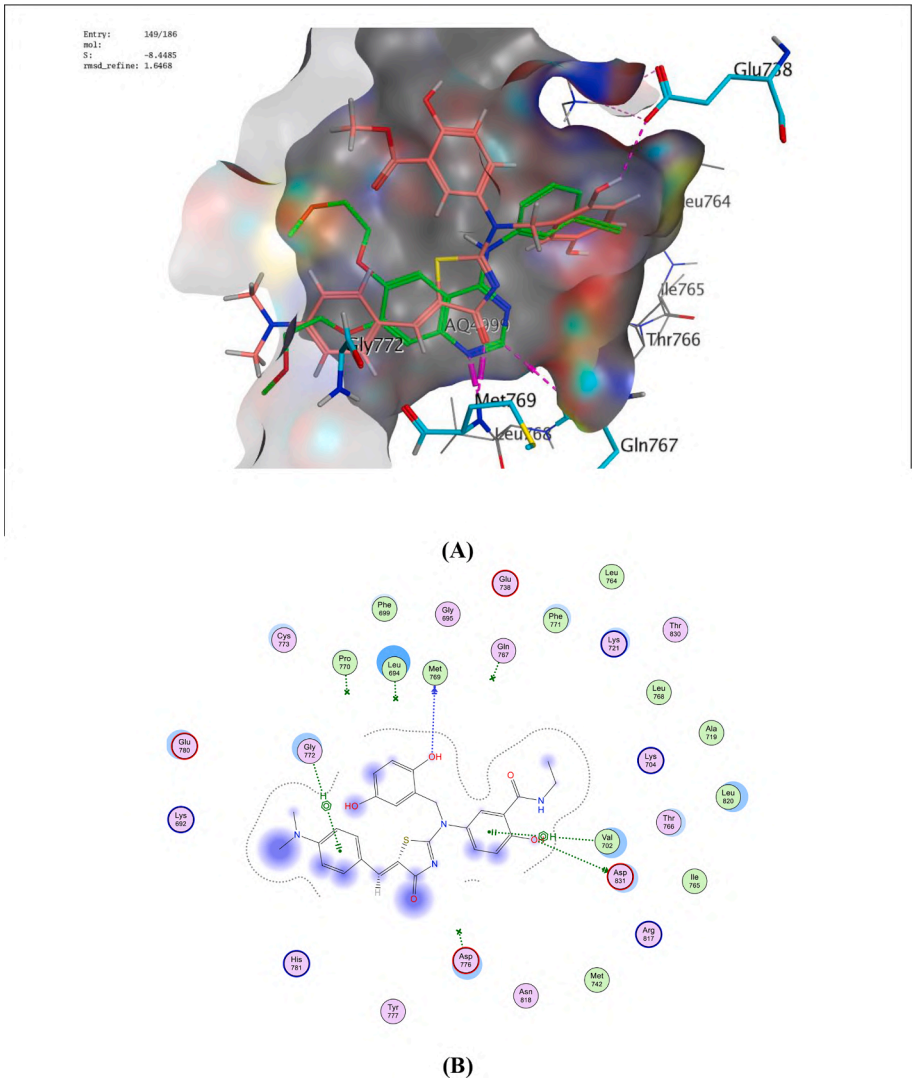

Fig. 6. (*continued*).

(KBr, ύ cm^{-1}): 3060, 2984, 2938, 1724, 1692, 1599, 1578, 1459, 1309, 1175, 1148, 998, 985, 750, 691; ^{1}H NMR (400 MHz, $CDCl_3$) δ = 7.58, 7.55 (dd, J = 11.5, 0.9 Hz, 1H; ═CH—CH═CH), 7.53–7.49 (m, 2H; ArH-2,6 cinnamyl), 7.41–7.35 (m, 3H; cinnamyl), 7.07 (d, J = 15.2 Hz, 1H; ═CH—CH═CH), 6.77, 6.73 (dd, J = 15.2, 11.5 Hz, 1H; ═CH—CH═CH), 4.28–4.20 (m, 4H; $2CH_2$), 1.30 (t, J = 7.2 Hz, 3H; CH_3). ^{13}C NMR (100 MHz, $CDCl_3$) δ 188.77, 178.78, 167.06, 144.72, 135.95, 135.53, 130.26, 129.12, 128.97, 127.88, 124.80, 77.48, 77.36, 77.16, 76.84, 62.60, 35.27, 14.18.

4.1.7. General method for synthesis of (Z)-(substituted)-5-(N-(2,5-dihydroxybenzyl)-N-(5-(substituted)-4-oxo-4,5-dihydrothiazol-2-yl) amino)-2-hydroxybenzamide ***(14a–c to 17a–c and 18a–b)***

The lavendustin C derivative (**6–9** or **10**) (1.5 mmol, 1.5 equiv.) was dissolved in 10 mL mixture of acetonitrile and ethanol (1:1) and stirred for 5 min before the appropriate rhodanine derivative (**RD4–6**) (1 mmol, 1 equiv.) was added. The reaction mixture was then stirred at 50–60 °C for 1–3 days until the rhodanine derivative was totally consumed as indicated by TLC. For derivatives of **RD4** and **RD6**, the solvent mixture was evaporated, and the product was recrystallized twice from firstly from aqueous ethanol and secondly from ethyl acetate/hexane. On the other hand, in case of compound **RD5**, the precipitated debenzylated side product was filtered. The filtrate was then left at room temperature to afford crystals of the target product that were filtered, dried at 50–60 °C in oven. *Rf* values were determined using a mobile phase of ethyl acetate: hexane (2:1).

4.1.7.1. Methyl (Z)-2-hydroxy-5-(N-(2,5-dihydroxybenzyl)-N-(5-(4-methylbenzylidenyl)-4-oxo-4,5-dihydrothiazol-2-yl)amino)benzoate ***(14a)***. Yellowish white crystal**;;** *Rf*: 0.38; yield: 65 %; m.p. 218–220 °C; IR (KBr, ύ cm^{-1}): 3360, 2950, 2853, 1683, 1603, 1541, 1508, 1336, 1291, 1182, 1089, 838, 789, 582; ^{1}H NMR (400 MHz, DMSO-d_6) δ = 10.73 (s, 1H; OH), 8.90 (s, 1H; OH), 8.71 (s, 1H; OH), 7.77 (d, J = 2.7 Hz 1H; ArH-6), 7.64 (s, 1H; ═CH), 7.46, 7.44 (dd, J = 8.7, 2.7 Hz, 1H; ArH-4), 7.36 (d, J = 8.1 Hz, 2H; ArH-2′,6′ 4-MeC_6H_4), 7.25 (d, J = 8.1 Hz, 2H; ArH-3′,5′ 4-MeC_6H_4), 7.05 (d, J = 8.7 Hz, 1H; ArH-3), 6.59 (d, J = 2.8 Hz, 1H; ArH-6″ benzyl), 6.58 (d, J = 8.8 Hz, 1H; ArH-3″ benzyl), 6.51, 6.49 (dd, J = 8.8, 2.7 Hz, 1H; ArH-4″ benzyl), 5.12 (s, 2H; CH_2 benzyl), 3.85 (s, 3H; —OCH_3), 2.29 (s, 3H, CH_3 4-MeC_6H_4); ^{13}C NMR (100 MHz, DMSO-d_6) δ = 179.69, 177.02, 167.66, 160.00, 149.77, 147.87, 140.06, 135.18, 131.22, 130.91, 130.72, 130.24, 129.90, 129.56, 128.19, 121.39, 118.78, 116.21, 116.13, 115.81, 114.46, 52.75, 52.69, 21.06. Analysis calc. for $C_{26}H_{22}N_2O_6S$ (490.53); C, 63.66; H, 4.52; N, 5.71; S, 6.54. Found: C, 63.52; H, 4.68; N, 5.79; S, 6.49.

4.1.7.2. Methyl (Z)-2-hydroxy-5-(N-(2,5-dihydroxybenzyl)-N-(5-(4-(dimethylamino)-benzylidenyl)-4-oxo-4,5-dihydrothiazol-2-yl)amino)benzoate ***(14b)***. Reaction solvent: acetonitrile; 50–60 °C for 6 days; Orange

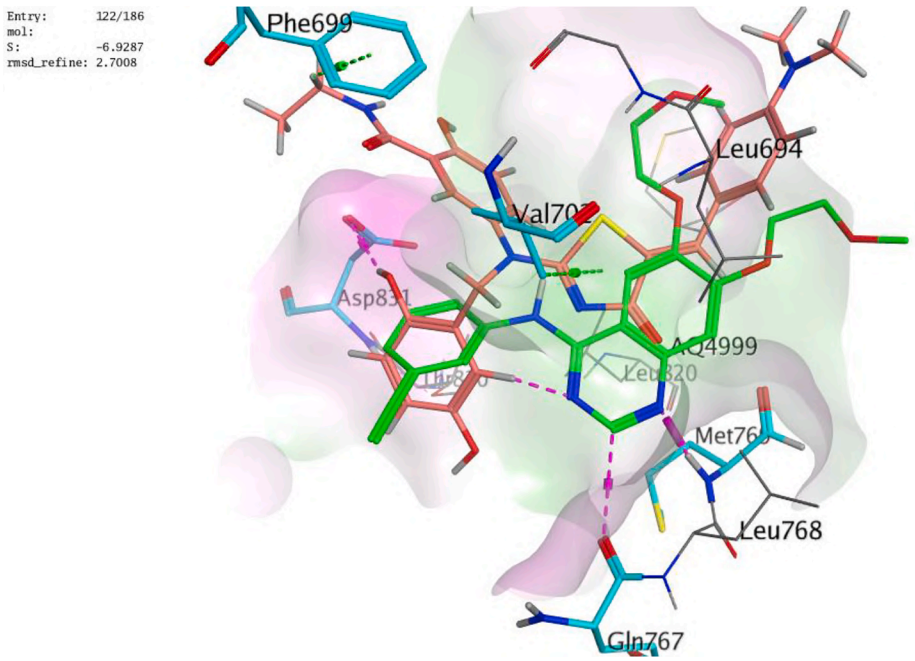

Fig. 7. Docking representation models within the binding site of EGFR; **(A)** Ligand interaction profile of compound **16b**; **(B)** 3D-docked model of compound **16b** (pink) overlapped with erlotinib (green).

red crystals; yield: 50 %; *Rf*: 0.26; m.p. 233.5–235 °C; IR (KBr, ύ cm^{-1}): 3456, 3297, 3066, 2949, 2805, 1675, 1614, 1577, 1526, 1445, 1372, 1284, 1189, 1167, 1015, 824, 798, 730; ^{1}H NMR (400 MHz, DMSO-d_6) δ = 10.74 (s, 1H; OH), 8.92 (s, 1H; OH), 8.72 (s, 1H; OH), 7.78 (d, J = 2.5 Hz, 1H; ArH-6), 7.56 (s, 1H; ═CH), 7.48, 7.46 (dd, J = 8.6, 2.5 Hz, 1H; ArH-4), 7.30 (d, J = 8.7 Hz, 2H; ArH-2′,6′ 4-Me$_2$NC$_6$H$_4$), 7.07 (d, J = 8.6 Hz 1H; ArH-3), 6.75 (d, J = 8.7 Hz, 2H; ArH-3′, 5′ 4-Me$_2$NC$_6$H$_4$), 6.64–6.57 (m, 2H; ArH-3″, 6″ benzyl), 6.52, 6.50 (dd, J = 8.5, 2.6 Hz, 1H; ArH-4″ benzyl), 5.11 (s, 2H; CH_2 benzyl), 3.87 (s, 3H; —O$\underline{CH_3}$), 2.95 (s, 6H, $(CH_3)_2$ 4-Me$_2$NC$_6$H$_4$); ^{13}C NMR (100 MHz, DMSO-d_6) δ = 180.55, 177.13, 168.13, 160.35, 151.61, 150.21, 148.24, 135.74, 132.19, 131.99, 131.84, 130.73, 122.88, 122.09, 120.91, 119.20, 116.62, 116.56, 116.14, 114.86, 112.53, 53.12, 52.88; Analysis calc. for $C_{27}H_{25}N_3O_6S$ (519.57); C, 62.42; H, 4.85; N, 8.09; S, 6.17. Found: C, 62.70; H, 4.91; N, 8.32; S, 6.25.

4.1.7.3. Methyl (Z)-2-hydroxy-5-(N-(2,5-dihydroxybenzyl)-N-(4-oxo-5-((E)-3-phenylallylidenyl)-4,5-dihydrothiazol-2-yl)amino)benzoate ***(14c)***. Yellowish white crystal;; *Rf*: 0.41; yield: 76 %; m.p. 173–175 °C; IR (KBr, ύ cm^{-1}): 3469, 3285, 3064, 2951, 1677, 1600, 1585, 1523, 1445, 1336, 1289, 1224, 1151, 1092, 972, 797, 732, 686; ^{1}H NMR (400 MHz, DMSO-d_6) δ = 10.73 (s, 1H; OH), 8.91 (s, 1H; OH), 8.73 (s, 1H; OH), 7.77 (d, J = 2.5 Hz, 1H; ArH-6), 7.61 (d, J = 7.2 Hz, 2H; ArH-6′,2′ cinnamyl), 7.48, 7.46 (dd, J = 8.8, 2.6 Hz, 1H; ArH-4), 7.37–7.30 (m, 4H; cinnamyl, ═CH—CH═CH), 7.16 (d, J = 15.4 Hz, 1H; ═CH—CH═$\underline{CH}$), 7.07 (d, J = 8.8 Hz, 1H; ArH-3), 6.94, 6.90 (dd, J = 15.4, 11.6 Hz, 1H; ═CH—$\underline{CH}$═CH), 6.63–6.57 (m, 2H; ArH-3″,6″ benzyl), 6.54–6.49 (m, 1H; ArH-4″ benzyl), 5.11 (s, 2H; CH_2 benzyl), 3.87 (s, 3H; —O$\underline{CH_3}$); ^{13}C NMR (100 MHz, DMSO-d_6) δ = 179.13, 176.42, 167.64, 160.00, 149.75, 147.81, 141,97, 135.83, 135.22, 131.74, 131.47, 130.43, 130.27, 129.25, 128.77, 127.62, 125.09, 121.48, 118.79, 116.15, 116.14, 115.74, 114.35, 52.67, 52.36; Analysis calc. for $C_{27}H_{22}N_2O_6S$ (502.54); C, 64.53; H, 4.41; N, 5.57; S, 6.38. Found: C, 64.78; H, 4.43; N, 5.73; S, 6.23.

4.1.7.4. (Z)-2-Hydroxy-5-(N-(2,5-dihydroxybenzyl)-N-(5-(4-methylbenzylidenyl)-4-oxo-4,5-dihydrothiazol-2-yl)amino)-N-methylbenzamide ***(15a)***. Yellowish white crystal; *Rf*: 0.26; yield: 73 %; m.p. 185–187 °C; IR (KBr, ύ cm^{-1}): 3453, 3372, 3191, 2941, 1680, 1652, 1598, 1531, 1366, 1296, 817, 734, 689; ^{1}H NMR (400 MHz, DMSO-d_6) δ = 12.90 (s, 1H; OH), 8.90 (s, 1H; OH), 8.81 (q, J = 4.9 Hz, 1H; $\underline{NH}CH_3$), 8.70 (s, 1H; OH), 7.93 (d, J = 2.4 Hz, 1H; ArH-6), 7.64 (s, 1H; ═CH), 7.37 (d, J = 8.3 Hz, 2H; ArH-2′,6′ 4-MeC$_6$H$_4$), 7.33, 7.30 (dd, J = 8.8, 2.4 Hz, 1H; ArH-4), 7.26 (d, J = 8.3 Hz, 2H; ArH-3′,5′ 4-MeC$_6$H$_4$), 6.96 (d, J = 8.8 Hz, 1H; ArH-3), 6.61 (d, J = 2.7 Hz, 1H; ArH-6″ benzyl), 6.58 (d, J = 8.7 Hz, 1H; ArH-3″ benzyl), 6.51, 6.49 (dd, J = 8.7, 2.7 Hz, 1H; ArH-4″ benzyl), 5.14 (s, 2H; CH_2 benzyl), 2.80 (d, J = 4.9 Hz, 3H; N$\underline{H}CH_3$ Methyl), 2.29 (s, 3H, CH_3 4-MeC$_6$H$_4$); ^{13}C NMR (100 MHz, DMSO-d_6) δ = 179.62, 177.10, 167.97, 160.21, 149.72, 147.77, 140.03, 133.17, 130.89, 130.84, 130.72, 129.90, 129.55, 129.01, 128.45, 128.15, 128.03, 121.38, 118.46, 116.19, 116.11, 115.75, 52.74, 26.07, 21.05; Analysis calc. for $C_{26}H_{23}N_3O_5S$ (489.55); C, 63.79; H, 4.74; N, 8.58; S, 6.55. Found: C, 63.51; H, 4.87; N, 8.79; S, 6.43.

4.1.7.5. (Z)-2-Hydroxy-5-(N-(2,5-dihydroxybenzyl)-N-(5-(4-(dimethylamino)benzylidenyl)-4-oxo-4,5-dihydrothiazol-2-yl)amino)-N-methylbenzamide ***(15b)***. Orange red crystal; *Rf*: 0.16 yield: 14 %; m.p. 219–221 °C; IR (KBr, ύ cm^{-1}): 3432, 3362, 3198, 2938, 2806, 1670, 1653, 1573, 1525, 1374, 1286, 1189, 835, 820, 755, 731, 521; ^{1}H NMR (400 MHz, DMSO-d_6) δ = 12.96 (s, 1H; OH), 8.95 (s, 1H; OH), 8.87 (q, J = 4.4 Hz 1H; $\underline{NH}CH_3$), 8.71 (s, 1H; OH), 7.96 (s, 1H; ArH-6), 7.57 (s, 1H; ═CH), 7.38–7.28 (m, 3H; ArH-2′,6′ 4-Me$_2$NC$_6$H$_4$, ArH-4), 6.98 (d, J = 8.7 Hz 1H; ArH-3), 6.76 (d, J = 8.8 Hz, 2H; ArH-3′,5′ 4-Me$_2$NC$_6$H$_4$), 6.63 (d, J = 2.7 Hz 1H; ArH-6″ benzyl), 6.60 (d, J = 8.7 Hz, 1H; ArH-3″ benzyl), 6.53, 6.51 (dd, J = 8.4, 2.7 Hz, 1H; ArH-4″ benzyl), 5.13 (s, 2H; CH_2 benzyl), 2.95 (s, 6H; $(CH_3)_2$ 4-Me$_2$NC$_6$H$_4$), 2.82 (d, J = 4.4 Hz, 3H; N$\underline{H}CH_3$ Methyl); ^{13}C NMR (100 MHz, DMSO-d_6) δ = 180.49, 177.24, 168.53, 160.72, 151.60, 150.20, 148.18, 133.74, 132.19, 131.84, 131.60, 128.52, 122.88, 122.13, 120.94, 118.94, 116.62, 116.58, 116.46, 116.12, 112.56, 52.93, 26.53; Analysis calc. for $C_{27}H_{26}N_4O_5S$ (518.59); C, 62.53; H, 5.05; N, 10.80; S, 6.18. Found: 62.70; H, 5.29; N, 11.07; S, 6.25.

4.1.7.6. (Z)-2-Hydroxy-5-(N-(2,5-dihydroxybenzyl)-N-(4-oxo-5-((E)-3-phenylallylidenyl)-4,5-dihydrothiazol-2-yl)amino)-N-methylbenzamide ***(15c)***. Yellowish white crystal; *Rf*: 0.22; yield: 51 %; m.p. 188–190 °C;

IR (KBr, ύ cm^{-1}): 3440, 3315, 2940, 1672, 1652, 1602, 1584, 1527, 1361, 1336, 1150, 963, 816, 746, 582; ^{1}H NMR (400 MHz, DMSO-d_6) δ = 12.96 (s, 1H; OH), 8.91 (s, 1H; OH), 8.85 (t, J = 4.5 Hz, 1H; NHCH$_3$), 8.71 (s, 1H; OH), 7.94 (d, J = 1.8 Hz, 1H; ArH-6), 7.60 (d, J = 7.5 Hz, 2H; ArH-2′,6′ cinnamyl), 7.37–7.28 (m, 5H; cinnamyl, =CH—CH=CH, ArH-4), 7.15 (d, J = 15.2 Hz, 1H; =CH—CH=CH), 6.98 (d, J = 8.7 Hz, 1H; ArH-3), 6.95, 6.92 (dd, J = 15.24, 11.5 Hz, 1H; =CH=CH=CH,), 6.62 (br, 1H; ArH-6″ benzyl), 6.58 (d, J = 8.4 Hz, 1H; ArH-3″ benzyl), 6.52, 6.50 (dd, J = 8.4, 1.9 Hz, 1H; ArH-4″ benzyl), 5.11 (s, 2H; CH$_2$ benzyl), 2.81 (d, J = 4.5 Hz, 3H; NHCH$_3$ Methyl); ^{13}C NMR (100 MHz, DMSO-d_6) δ = 179.56, 177.04, 168.53, 160.81, 150.20, 148.22, 142.48, 136.30, 133.67, 132.16, 131.56, 130.97, 129.72, 129.23, 128.51, 128.11, 125.54, 121.98, 118.97, 116.66, 116.60, 116.39, 116.19, 52.88, 26.53; Analysis calc. for $C_{27}H_{23}N_3O_5S$ (501.56); C, 64.66; H, 4.62; N, 8.38; S, 6.39. Found: C, 64.49; H, 4.80; N, 8.60; S, 6.47.

4.1.7.7. (Z)-N-Ethyl-2-hydroxy-5-(N-(2,5-dihydroxybenzyl)-N-(5-(4-methylbe'zylidenyl)-4-oxo-4,5-dihydrothiazol-2-yl)amino)benzamide ***(16a)***. Yellowish white crystal; *Rf*: 0.32; yield: 67 %; m.p. 203–205 °C; IR (KBr, ύ cm^{-1}): 3332, 3079, 2976, 2934, 1676, 1644, 1601, 1541, 1492, 1359, 1335, 1299, 1181, 1147, 833, 813, 750, 612; ^{1}H NMR (400 MHz, DMSO-d_6) δ = 12.97 (s, 1H; OH), 8.90 (s, 1H; OH), 8.83 (t, J = 5.4 Hz, 1H; NHCH$_2$), 8.70 (s, 1H; OH), 7.99 (d, J = 2.4 Hz, 1H; ArH-6), 7.65 (s, 1H; =CH), 7.37 (d, J = 8.2 Hz, 2H; ArH-2″,6″ 4-MeC$_6$H$_4$), 7.30, 7.28 (dd, J = 8.7, 2.4 Hz, 1H; ArH-4), 7.26 (d, J = 8.2 Hz, 2H; ArH-3″,5″ 4-MeC$_6$H$_4$), 6.95 (d, J = 8.7 Hz, 1H; ArH-3), 6.62 (d, J = 2.8 Hz, 1H; ArH-6″ benzyl), 6.58 (d, J = 8.7 Hz, 1H; ArH-3″ benzyl), 6.51, 6.49 (dd, J = 8.7, 2.8 Hz, 1H; ArH-4″ benzyl), 5.14 (s, 2H; CH$_2$ benzyl), 3.32–3.27 (m, 2H; NHCH$_2$ Ethyl), 2.29 (s, 3H, CH$_3$ 4-MeC$_6$H$_4$), 1.13 (t, J = 7.2 Hz, 3H; CH$_2$CH$_3$ Ethyl); ^{13}C NMR (100 MHz, DMSO-d_6) δ = 180.08, 177.58, 167.88, 160.90, 150.19, 148.22, 140.49, 133.69, 131.34, 131.26, 131.17, 130.36, 130.01, 128.61, 128.47, 121.85, 118.90, 116.59, 116.54, 116.18, 53.22, 34.53, 21.50, 14.82; Analysis calc. for $C_{27}H_{25}N_3O_5S$ (503.57); C, 64.40; H, 5.00; N, 8.34; S, 6.37. Found: C, 64.57; H, 5.16; N, 8.61; S, 6.41.

4.1.7.8. (Z)-N-Ethyl-2-hydroxy-5-(N-(2,5-dihydroxybenzyl)-N-(5-(4-(dimethylamino)-benzylidenyl)-4-oxo-4,5-dihydrothiazol-2-yl)amino)benzamide ***(16b)***. Orange crystal; *Rf*: 0.22; yield: 12 %; m.p. 203–205 °C; IR (KBr, ύ cm^{-1}): 3328, 3085, 2932, 1674, 1641, 1580, 1530, 1362, 1292, 1184, 1168, 1012, 816, 754, 686; ^{1}H NMR (400 MHz, DMSO-d_6) δ = 13.00 (s, 1H; OH), 8.94 (s, 1H; OH), 8.86 (brs, 1H; NHCH$_2$), 8.71 (s, 1H; OH), 8.01 (s, 1H; ArH-6), 7.56 (s, 1H; =CH), 7.36–7.27 (m, 3H; ArH-2′,6′ 4-Me$_2$NC$_6$H$_4$, ArH-4), 6.97 (d, J = 8.9 Hz, 1H; ArH-3), 6.76 (d, J = 8.3 Hz, 2H; ArH-3′,5′ 4-Me$_2$NC$_6$H$_4$), 6.62 (s, 1H; ArH-6″ benzyl), 6.59 (d, J = 8.6 Hz, 1H; ArH-3″ benzyl), 6.51 (d, J = 8.6 Hz, 1H; ArH-4″ benzyl), 5.13 (s, 2H; CH$_2$ benzyl), 3.32–3.28 (m, 2H; NHCH$_2$ Ethyl), 2.95 (s, 6H, (CH$_3$)$_2$ 4-Me$_2$NC$_6$H$_4$), 1.15 (t, J = 7.2 Hz, 3H; CH$_2$CH$_3$ Ethyl); ^{13}C NMR (100 MHz, DMSO-d_6) δ = 180.48, 177.27, 167.99, 160.88, 151.62, 150.21, 148.16, 133.83, 132.20, 131.85, 131.60, 128.50, 122.88, 122.14, 120.93, 118.89, 116.62, 116.52, 116.42, 116.10, 112.57, 52.94, 34.53, 14.81; Analysis calc. for $C_{28}H_{28}N_4O_5S$ (532.62); C, 63.14; H, 5.30; N, 10.52; S, 6.02. Found: C, 63.40; H, 5.41; N, 10.78; S, 6.19.

4.1.7.9. (Z)-N-Ethyl-2-hydroxy-5-(N-(2,5-dihydroxybenzyl)-N-(4-oxo-5-((E)-3-phenylallylidenyl)-4,5-dihydrothiazol-2-yl)amino)benzamide ***(16c)***. Yellowish white crystal; *Rf*: 0.30; yield: 30 %; m.p. 171–173 °C; IR (KBr, ύ cm^{-1}): 3346, 3067, 2975, 2935, 1676, 1644, 1602, 1585, 1536, 1354, 1298, 1256, 1229, 1148, 963, 838, 744, 688; ^{1}H NMR (400 MHz, DMSO-d_6) δ = 13.02 (s, 1H; OH), 8.93 (s, 1H; OH), 8.87 (t, J = 5.5 Hz, 1H; NHCH$_2$), 8.72 (s, 1H; OH), 7.99 (d, J = 2.4 Hz, 1H; ArH-6), 7.62 (d, J = 8.2 Hz, 2H; ArH-2′,6′ cinnamyl), 7.40–7.27 (m, 5H; cinnamyl, =CH—CH=CH, ArH-4), 7.16 (d, J = 15.4 Hz, 1H; =CH—CH=CH), 6.99–6.91 (m, 2H; =CH—CH=CH, ArH-3), 6.63 (d, J = 2.6 Hz, 1H; ArH-6″ benzyl), 6.59 (d, J = 8.6 Hz, 1H; ArH-3″ benzyl), 6.53, 6.51 (dd, J = 8.6, 2.6 Hz, 1H; ArH-4″ benzyl), 5.12 (s, 2H; CH$_2$ benzyl), 3.33–3.28 (m, 2H; NHCH$_2$ Ethyl), 1.15 (t, J = 7.2 Hz, 3H; CH$_2$CH$_3$ Ethyl); ^{13}C NMR (100 MHz, DMSO-d_6) δ = 179.57, 177.09, 167.96, 161.02, 150.21, 148.21, 142.50, 136.29, 133.76, 132.16, 131.52, 130.97, 129.72, 129.23, 128.52, 128.11, 125.54, 121.98, 118.95, 116.63, 116.60, 116.40, 116.19, 52.89, 34.54, 14.82; Analysis calc. for $C_{28}H_{25}N_3O_5S$ (515.58); C, 65.23; H, 4.89; N, 8.15; S, 6.22. Found: C, 65.02; H, 5.06; N, 8.42; S, 6.15.

4.1.7.10. (Z)-N-Butyl-2-hydroxy-5-(N-(2,5-dihydroxybenzyl)-N-(5-(4-methylbenzylidenyl)-4-oxo-4,5-dihydrothiazol-2-yl)amino)benzamide ***(17a)***. Yellowish white crystal; R_f 0.38; yield: 63 %; m.p. 210–212 °C; IR (KBr, ύ cm^{-1}): 3489, 3381, 3259, 2961, 2933, 2860, 1676, 1650, 1598, 1533, 1363, 1302, 1287, 1186, 1013, 828, 729, 688, 565; ^{1}H NMR (400 MHz, DMSO-d_6) δ = 12.97 (s, 1H; OH), 8.91 (s, 1H; OH), 8.80 (t, J = 5.4 Hz, 1H; NHCH$_2$), 8.71 (s, 1H; OH), 7.99 (d, J = 2.4 Hz, 1H; ArH-6), 7.66 (s, 1H; =CH), 7.38 (d, J = 8.0 Hz, 2H; ArH-2′,6′ 4-MeC$_6$H$_4$), 7.34, 7.32 (dd, J = 8.6, 2.4 Hz, 1H; ArH-4), 7.27 (d, J = 8.0 Hz, 2H; ArH-3′,5′ 4-MeC$_6$H$_4$), 6.97 (d, J = 8.6 Hz, 1H; ArH-3), 6.63 (d, J = 2.8 Hz, 1H; ArH-6″ benzyl), 6.59 (d, J = 8.6 Hz, 1H; ArH-3″ benzyl), 6.52, 6.50 (dd, J = 8.6, 2.8 Hz, 1H; ArH-4″ benzyl), 5.16 (s, 2H; CH$_2$ benzyl), 3.32–3.26 (m, 2H; NHCH$_2$ Butyl), 2.30 (s, 3H, CH$_3$ 4-MeC$_6$H$_4$), 1.57–1.47 (m, 2H; NHCH$_2$CH$_2$ Butyl), 1.38–1.27 (m, 2H, CH$_2$CH$_2$CH$_2$ Butyl), 0.89 (t, J = 7.2 Hz, 3H; CH$_3$ Butyl); ^{13}C NMR (100 MHz, DMSO-d_6) δ = 180.07, 177.57, 167.98, 160.84, 150.21, 148.21, 140.48, 133.65, 131.34, 131.28, 131.15, 130.35, 130.00, 128.62, 128.49, 121.86, 118.90, 116.56, 116.53, 116.16, 53.19, 31.22, 21.50, 20.07, 14.11; Analysis calc. for $C_{29}H_{29}N_3O_5S$ (531.63); C, 65.52; H, 5.50; N, 7.90; S, 6.03. Found: C, 65.78; H, 5.63; N, 8.14; S, 6.09.

4.1.7.11. (Z)-N-Butyl-2-hydroxy-5-(N-(2,5-dihydroxybenzyl)-N-(5-(4(dimethylamino) benzylidenyl)-4-oxo-4,5-dihydrothiazol-2-yl)amino) benzamide ***(17b)***. Orange red crystal; *Rf*: 0.29; yield: 15 %; m.p. 220–223 °C; IR (KBr, ύ cm^{-1}): 3489, 3382, 3260, 2961, 2934, 2860, 1676, 1650, 1598, 1534, 1391, 1363, 1302, 1287, 1186, 1013, 828, 729, 688, 565; ^{1}H NMR (400 MHz, DMSO-d_6) δ = 12.98 (s, 1H; OH), 8.92 (s, 1H; OH), 8.81 (t, J = 5.5 Hz, 1H; NHCH$_2$), 8.69 (s, 1H; OH), 7.99 (d, J = 2.6 Hz, 1H; ArH-6), 7.56 (s, 1H; =CH), 7.34–7.28 (m, 3H; ArH-2′,6′ 4-Me$_2$NC$_6$H$_4$, ArH-4), 6.96 (d, J = 8.8 Hz, 1H; ArH-3), 6.75 (d, J = 8.8 Hz, 2H; ArH-3′,5′ 4-NMe$_2$C$_6$H$_4$), 6.61 (d, J = 2.8 Hz, 1H; ArH-6″ benzyl), 6.57 (d, J = 8.6 Hz, 1H; ArH-3″ benzyl), 6.51, 6.49 (dd, J = 8.6, 2.8 Hz, 1H; ArH-4″ benzyl), 5.12 (s, 2H; CH$_2$ benzyl), 3.32–3.25 (m, 2H; NHCH$_2$ Butyl), 2.94 (s, 6H, (CH$_3$)$_2$ 4-Me$_2$NC$_6$H$_4$), 1.55–1.46 (m, 2H; NHCH$_2$CH$_2$ Butyl), 1.36–1.27 (m, 2H, CH$_2$CH$_2$CH$_2$ Butyl), 0.89 (t, J = 7.3 Hz, 3H; CH$_3$ Butyl); ^{13}C NMR (100 MHz, DMSO-d_6) δ = 180.48, 177.25, 168.07, 160.84, 151.62, 150.22, 148.15, 134.10, 133.77, 132.17, 131.85, 131.60, 128.52, 122.90, 122.15, 120.94, 118.90, 116.60, 116.49, 116.45, 116.07, 112.57, 111.37, 52.91, 39.23, 31.23, 20.08, 14.12; Analysis calc. for $C_{30}H_{32}N_4O_5S$ (560.67); C, 64.27; H, 5.75; N, 9.99; S, 5.72. Found: C, 64.43; H, 5.92; N, 10.13; S, 5.81.

4.1.7.12. (Z)-N-Butyl-2-hydroxy-5-(N-(2,5-dihydroxybenzyl)-N-(4-oxo-5-((E)-3-phenylallylidenyl)-4,5-dihydrothiazol-2-yl)amino)benzamide ***(17c)***. Yellowish white crystal; *Rf*: 0.36; yield: 60 %; m.p. 172–175 °C; IR (KBr, ύ cm^{-1}): 3359, 3066, 2954, 2928, 2864, 1675, 1646, 1604, 1586, 1538, 1498, 1455, 1355, 1303, 1233, 1147, 964, 845, 742, 683.

^{1}H NMR (400 MHz, DMSO-d_6) δ = 13.00 (s, 1H; OH), 8.92 (s, 1H; OH), 8.83 (t, J = 5.5 Hz, 1H; NHCH$_2$), 8.72 (s, 1H; OH), 7.99 (d, J = 2.1 Hz, 1H; ArH-6), 7.62 (d, J = 7.7 Hz, 2H; ArH-2′,6′ cinnamyl), 7.39–7.27 (m, 5H; cinnamyl, =CH—CH=CH, ArH-4), 7.17 (d, J = 15.4 Hz, 1H; =CH—CH=CH), 7.00–6.91 (m, 2H; =CH—CH=CH, ArH-3), 6.63 (d, J = 2.39 Hz, 1H; ArH-6″ benzyl), 6.59 (d, J = 8.6 Hz, 1H; ArH-3″ benzyl), 6.53, 6.51 (dd, J = 8.6, 2.6 Hz, 1H; ArH-4″ benzyl), 5.12 (s, 2H; CH$_2$ benzyl), 3.32–3.26 (m, 2H; NHCH$_2$ Butyl), 1.57–1.47 (m, 2H; NHCH$_2$CH$_2$ Butyl), 1.38–1.28 (m, 2H, CH$_2$CH$_2$CH$_2$ Butyl), 0.91 (t, J =

7.2 Hz, 3H; CH_3 Butyl); ^{13}C NMR (100 MHz, DMSO-d_6) δ = 179.56, 177.07, 168.03, 160.95, 150.22, 148.20, 142.48, 136.30, 133.74, 132.19, 131.53, 130.94, 129.72, 129.23, 128.56, 128.11, 125.55, 122.00, 118.93, 116.59, 116.44, 116.16, 52.87, 31.25, 20.09, 14.12; Analysis calc. for $C_{30}H_{29}N_3O_5S$ (543.64); C, 66.28; H, 5.38; N, 7.73; S, 5.90. Found: C, 66.05; H, 5.49; N, 7.97; S, 5.84.

4.1.7.13. (Z)-N-(4-Chlorophenyl)-2-hydroxy-5-(N-(2,5-dihydroxybenzyl)-N-(5-(4-methylbenzylidenyl)-4-oxo-4,5-dihydrothiazol-2-yl)amino)benzamide ***(18a)***. Yellowish white crystal; *Rf*: 0.29; yield: 10 %; m.p. charring 252–254 °C; IR (KBr, ύ cm^{-1}): 3424, 3353, 2973, 1673, 1652, 1599, 1545, 1496, 1361, 1281, 1202, 807, 826, 693; ^1H NMR (400 MHz, DMSO-d_6) δ = 12.03 (s, 1H; OH), 10.45 (s, 1H; NH), 8.92 (s, 1H; OH), 8.71 (s, 1H; OH), 7.98 (d, J = 2.4 Hz, 1H; ArH-6), 7.73 (d, J = 8.6 Hz, 2H; ArH-3′,5′ 4-ClC_6H_4), 7.64 (s, 1H; =CH), 7.42 (d, J = 8.6 Hz, 2H; ArH-2′,6′, 4-ClC_6H_4), 7.40–7.35 (m, 3H; ArH-2″,6″ 4-MeC_6H_4, ArH-4), 7.25 (d, J = 7.8 Hz, 2H; ArH-3″,5″ 4-MeC_6H_4), 7.04 (d, J = 8.7 Hz, 1H; ArH-3), 6.62 (d, J = 2.2 Hz, 1H; ArH-6‴ benzyl), 6.59 (d, J = 8.6 Hz, 1H; ArH-3‴ benzyl), 6.51, 6.49 (dd, J = 8.6, 2.2 Hz, 1H; ArH-4‴ benzyl), 5.16 (s, 2H; CH_2 benzyl), 2.29 (s, 3H; CH_3 4-MeC_6H_4); ^{13}C NMR (100 MHz, DMSO-d_6) δ = 179.62, 177.07, 164.62, 158.25, 149.74, 147.71 139.99, 137.04, 133.11, 131.32, 130.90, 130.65, 129.86, 129.51, 129.37, 128.70, 128.22, 127.88, 122.24, 121.44, 119.31, 118.20, 116.07, 115.93, 115.62, 52.84, 21.03; Analysis calc. for $C_{31}H_{24}ClN_3O_5S$ (586.06); C, 63.53; H, 4.13; N, 7.17; S, 5.47. Found: C, 63.64; H, 4.20; N, 7.41; S, 5.60.

4.1.7.14. (Z)-N-(4-Chlorophenyl)-2-hydroxy-5-(N-(2,5-dihydroxybenzyl)-N-(5-(4-dimethylamino)-benzylidenyl)-4-oxo-4,5-dihydrothiazol-2-yl)amino)benzamide ***(18b)***. Red crystal; *Rf*: 0.24; yield: 10 %; m.p. 233–235 °C; IR (KBr, ύ cm^{-1}): 3313, 2925, 2855, 1675, 1651, 1609, 1579, 1537, 1495, 1361, 1183, 1168, 1014, 811, 523; ^1H NMR (400 MHz, DMSO-d_6) δ = 12.05 (s, 1H; OH), 10.45 (s, 1H; NH), 9.25–8.31 (m, 2H; OH), 7.99 (d, J = 2.0 Hz, 1H; ArH-6), 7.73 (d, J = 8.6 Hz, 2H; ArH-3′,5′ 4-ClC_6H_4), 7.56 (s, 1H; =CH), 7.46–7.36 (m, 3H; ArH-2′,6′, 4-ClC_6H_4, ArH-4), 7.30 (d, J = 8.6 Hz, 2H; ArH-2″,6″ 4-$Me_2NC_6H_4$), 7.06 (d, J = 8.6 Hz, 1H; ArH-3), 6.74 (d, J = 8.6 Hz, 2H; ArH-3″,5″ 4-$Me_2NC_6H_4$), 6.63 (d, J = 2.3 Hz, 1H; ArH-6‴ benzyl), 6.58 (d, J = 8.3 Hz, 1H; ArH-3‴ benzyl), 6.51, 6.49 (dd, J = 8.5, 2.5 Hz, 1H; ArH-4‴ benzyl), 5.14 (s, 2H; CH_2 benzyl), 2.94 (s, 6H; $(CH_3)_2$ 4-$Me_2NC_6H_4$); ^{13}C NMR (100 MHz, DMSO-d_6) δ = 180.26, 176.91, 164.80, 158.19, 151.28, 149.84, 147.81, 137.07, 133.41, 131.91, 131.85, 131.51, 129.56, 128.85, 128.11, 122.53, 122.46, 121.84, 120.56, 119.29, 118.31, 116.27, 116.06, 115.69, 112.20, 52.69; Analysis calc. for $C_{32}H_{27}ClN_4O_5S$ (615.10); C, 62.49; H, 4.42; N, 9.11; S, 5.21. Found: C, 62.67; H, 4.53; N, 9.34; S, 5.34.

4.2. Biology

4.2.1. Cytotoxic activity using SRB assay and evaluation of IC_{50}

MCF7, MDA-MB-231 (breast cancer), colon HCT-116, lung A549, cervix HeLa, Jurkat leukemia and U937 Histiocytic lymphoma cell lines were maintained in the Molecular Pharmacology lab (Sharjah institute for Medical Research, University of Sharjah, United Arab Emirates). Cells were cultured in DMEM and RPMI media supplemented with 10 % heat-inactivated FBS, 50 units/mL of penicillin and 50 g/mL of streptomycin (all from Sigma) and cells were maintained at 37 °C in a humidified atmosphere containing 5 % CO_2. The cells were maintained as a "monolayer culture" by serial subculturing. Cytotoxicity was determined using the SRB method as previously described [44]. Exponentially growing cells were collected using 0.25 % trypsin-EDTA and seeded in 96-well plates at 1000–2000 cells/well in supplemented DMEM medium. After 24 h, cells were incubated for 48 h with various concentrations of the tested compounds as well as DMSO, and doxorubicin as the negative and positive reference standards. At the end of the treatment period, the cells were fixed with 50 % trichloroacetic acid for 1 h at 4 °C. Wells were stained for 10 min at room temperature with 0.4 % SRB dissolved in 1 % acetic acid. After washing, the plates were air dried for 24 h, and the dye was solubilized with Tris HCl for 5 min on a shaker at 1600 rpm. The optical density (OD) of each well was measured spectrophotometrically at 564 nm with an ELISA microplate reader (Meter tech. S960, USA). The IC_{50} values were calculated according to the equation for Boltzmann sigmoidal concentration response curve using the nonlinear regression models (GraphPad, Prism Version 5). The results reported are means of at least three separate experiments. Significant differences were analyzed by one-way ANOVA wherein the differences were significant at $P < 0.05$. Control (untreated cells) were incubated in DMSO equal to the highest concentration used to dissolve the compounds. The concentration of DMSO did not exceed 0.1 % in all samples.

4.2.2. Cell cycle analysis

4.2.2.1. Cell culture. HeLa: Cervical Cancer was obtained from Nawah Scientific Inc., (Mokatam, Cairo, Egypt).

Cells were maintained in RPMI media supplemented with 100 mg/mL of streptomycin, 100 units/mL of penicillin and 10 % of heat-inactivated fetal bovine serum in humidified, 5 % (v/v) CO_2 atmosphere at 37 °C.

4.2.2.2. Flow cytometry assay. After treatment with test compounds for the specified duration, cells (10^5 cells) were collected by trypsinization and washed twice with ice-cold PBS (pH 7.4). Cells were resuspended in two milliliters of 60 % ice-cold ethanol and incubated at 4 °C for 1 h for fixation. Fixed cells were washed twice again with PBS (pH 7.4) and re-suspended in 1 mL of PBS containing 50 μg/mL RNAase A and 10 μg/mL propidium iodide (PI). After 20 min of incubation in dark at 37 °C, cells were analyzed for DNA contents using flow cytometric analysis using FL2 (λex/em 535/617 nm) signal detector (ACEA Novocyte™ flow cytometer, ACEA Biosciences Inc., San Diego, CA, USA). For each sample, 12,000 events are acquired. Cell cycle distribution was calculated using ACEA NovoExpress™ software (ACEA Biosciences Inc., San Diego, CA, USA) [45].

4.2.2.3. Cell apoptosis assay. Flow cytometry cell apoptosis analysis was conducted to examine the apoptotic effect of the synthesized compounds using the Annexin V-FITC cell apoptosis detection kit (Biovision, K101-25). First, HeLa cells at a density of 2×10^5 were seeded in 6-well plates and incubated for 24 h. The cells were then treated with 1.9 μM compound **14b** for 24 h. The treated cells were detached with trypsin (5 min, 37 °C), collected by centrifugation (1–5 x 10^5), washed twice with PBS, and resuspended in 500 μL of a 1X binding buffer. Cells were double-stained with 5 μL Annexin V-FITC and 5 μL PI in the dark at room temperature for 5 min. Annexin V-FITC binding was analyzed by flow cytometry (Ex = 488 nm; Em = 530 nm) using BD FACSCalibur flow cytometer (BD Bioscience) and FITC signal detector (usually FL1) and PI staining by the phycoerythrin emission signal detector (usually FL2) [46].

4.2.3. EGFR enzyme assay

Inhibition of EGFR was evaluated using EGFR kinase assay kit (Bioscience). It is designed to measure EGFR activity for the purpose of screening via Kinase-Glo® MAX as a reagent for detection [45]. By comparing test compounds to control, percent inhibition was calculated. The value of inhibitory concentration (IC_{50}) was attained by the concentration-inhibition response curve compared to reference drug (erlotinib). The kinase profiling assay protocol was done according to the manufacturer's instructions (6405 Mira Mesa Blvd. Suite 100 San Diego, CA 92121, USA). In this system, the master mixture (25 μL per well) was prepared using 6 μL 5x Kinase assay buffer + 1 μL ATP (500

μM) + 1 μL 50x PTK substrate + 17 μL water, respectively. 5 μL of inhibitor solution **14a, 14b** or **16b** was added to each of wells labeled as "Test Inhibitor". For the "Positive Control" and "Blank", 5 μL of the same solution without inhibitor (Inhibitor buffer) were added. The kinase reaction was initiated by adding 20 μL of diluted EGFR enzyme to the wells designated "Positive Control" and "Test Inhibitor Control". After 40 min incubation at 30 °C 50 μL of Kinase-Glo Max reagent were added to each well. The plate was covered with aluminum foil and incubated at room temperature for 15 min followed by measurement of luminescence using the microplate reader (Tecan Spark Reader). The IC_{50} values of tested compounds required to decrease the kinase activity by 50 % were calculated against reference drug erlotinib [47].

4.3. Molecular docking simulations

The molecular Operating Environment (MOE-2014) software package was used for running molecular docking simulations. Test compounds were drawn using ChemDraw Ultra (8, 2016) and their energy were minimized using MMFF94x Forcefield energy minimization capability of MOE software with a gradient RMS of 0.0001 Kcal/mol/A^2 and prepared ligands were saved as Microsoft Access Data Base (mdb) file. Crystal structures of target protein: EGFR (PDB ID: 1 M17 was downloaded from RCSB Protein Data Bank website (https://www.rcsb.org/). The protein was prepared in MOE program using protein Quick prep capability to protonate its structure and remove water molecules. Validation of prepared protein was performed by docking its co-crystallized ligands (Erlotinib) and docking score (S; Kcal/mol) and RMSD (Å) were in-agreement to the reported (Informatics in Medicine Unlocked 26 (2021) 100748 and www.pnas.org/cgi/doi/https://doi.org/10.1073/pnas.1525047113). The prepared ligand was docked into active site using MOE Alpha triangle placement method and refinements were done by Forcefield and scored using affinity δG (S; Kcal/mol) scoring system and listed in Table 5. Docking poses of ligands with best docking score and/or lowest RMSD values were inspected for their binding interactions as shown in Fig. 5.

CRediT authorship contribution statement

Shimaa A. Othman: Writing – original draft, Visualization, Validation, Methodology, Investigation, Formal analysis, Data curation. **Ola F. Abou-Ghadir:** Writing – review & editing, Validation, Supervision, Resources. **Varsha Menon:** Writing – original draft, Visualization, Methodology, Investigation. **Wafaa S. Ramadan:** Writing – original draft, Visualization, Methodology, Investigation. **Yaser A. Mostafa:** Writing – review & editing, Supervision. **Raafat El-Awady:** Writing – review & editing, Supervision, Software, Resources, Project administration, Funding acquisition, Formal analysis, Data curation. **Hajjaj H. M. Abdu-Allah:** .

Declaration of competing interest

The authors declare that they have no known competing financial interests or personal relationships that could have appeared to influence the work reported in this paper.

Acknowledgements

This work was supported by Faculty of pharmacy, Assiut University, Assiut Egypt.

Appendix A. Supplementary material

Supplementary data to this article can be found online at https://doi.org/10.1016/j.bioorg.2024.107884.

Data availability

Data will be made available on request.

References

[1] M.E. J. Ferlay, F. Lam, M. Colombet, L. Mery, M. Pineros, A. Znaor, I. Soerjomataram, F. Bray, Global Cancer Observatory: Cancer Today, 2024, Available from: https://gco.iarc.who.int/today.
[2] https://www.who.int/news-room/fact-sheets/detail/cancer (10/2/2022).
[3] H. Sung, J. Ferlay, R.L. Siegel, M. Laversanne, I. Soerjomataram, A. Jemal, F. Bray, Global Cancer Statistics 2020: GLOBOCAN estimates of incidence and mortality worldwide for 36 cancers in 185 countries, CA Cancer J. Clin. 71 (2021) (2020) 209–249.
[4] S. Fortin, G. Bérubé, Advances in the development of hybrid anticancer drugs, Expert Opin. Drug Discov. 8 (2013) 1029–1047.
[5] E. Sflakidou, G. Leonidis, E. Foroglou, C. Siokatas, V. Sarli, Recent advances in natural product-based hybrids as anti-cancer agents, Molecules 27 (2022) 6632.
[6] E. Kucuksayan, T. Ozben, Hybrid compounds as multitarget directed anticancer agents, Curr. Top. Med. Chem. 17 (2017) 907–918.
[7] M. Szumilak, A. Wiktorowska-Owczarek, A. Stanczak, Hybrid drugs—a strategy for overcoming anticancer drug resistance? Molecules 26 (2021) 2601.
[8] K. Nepali, S. Sharma, M. Sharma, P. Bedi, K. Dhar, Rational approaches, design strategies, structure activity relationship and mechanistic insights for anticancer hybrids, Eur. J. Med. Chem. 77 (2014) 422–487.
[9] X. Li, X. Li, F. Liu, S. Li, D. Shi, Rational multitargeted drug design strategy from the perspective of a medicinal chemist, J. Med. Chem. 64 (2021) 10581–10605.
[10] N. Kerru, P. Singh, N. Koorbanally, R. Raj, V. Kumar, Recent advances (2015–2016) in anticancer hybrids, Eur. J. Med. Chem. 142 (2017) 179–212.
[11] M. Brindisi, S.M. Kessler, V. Kumar, C. Zwergel, Multi-target directed ligands for the treatment of cancer, Front. Oncol. 12 (2022) 980141.
[12] A.R. Niederriter, A. Varshney, S.C. Parker, D.M. Martin, Super enhancers in cancers, complex disease, and developmental disorders, Genes 6 (2015) 1183–1200.
[13] P. Roszczenko, S. Holota, O.K. Szewczyk, R. Dudchak, K. Bielawski, A. Bielawska, R. Lesyk, 4-Thiazolidinone-bearing hybrid molecules in anticancer drug design, Int. J. Mol. Sci. 23 (2022) 13135.
[14] D. Havrylyuk, B. Zimenkovsky, O. Vasylenko, A. Gzella, R. Lesyk, Synthesis of new 4-thiazolidinone-, pyrazoline-, and isatin-based conjugates with promising antitumor activity, J. Med. Chem. 55 (2012) 8630–8641.
[15] H.H.M. Abdu Allah, A.N.A. El Shorbagi, 5-Aminosalyclic acid (5-ASA): a unique anti-inflammatory salicylate, Med. Chem. 06 (2016) 306–315.
[16] W.S. Ramadan, M.M. Saber-Ayad, E. Saleh, H.H.M. Abdu-Allah, A.A. El-Shorbagi, V. Menon, H. Tarazi, M.H. Semreen, N.C. Soares, S. Hafezi, T. Venkatakhalam, S. Ahmed, O. Kanie, R. Hamoudi, R. El-Awady, Design, synthesis and mechanistic anticancer activity of new acetylated 5-aminosalicylate-thiazolinone hybrid derivatives, iScience. 27 (2024) 108659.
[17] W.S. Ramadan, E.M. Saleh, V. Menon, C.G. Vazhappilly, H.H.M. Abdu-Allah, A.N. A. El-Shorbagi, W. Mansour, R. El-Awady, Induction of DNA damage, apoptosis and cell cycle perturbation mediate cytotoxic activity of new 5-aminosalicylate-4-thiazolinone hybrid derivatives, Biomed. Pharmacother. 131 (2020) 110571.
[18] S.A. Othman, O.F. Abou-Ghadir, W.S. Ramadan, Y.A. Mostafa, R. El-Awady, H.H. M. Abdu-Allah, The design, synthesis, biological evaluation, and molecular docking of new 5-aminosalicylamide-4-thiazolinone hybrids as anticancer agents, Archiv. Pharm. 356 (2023) e2300315.
[19] C.G. Vazhappilly, E. Saleh, W. Ramadan, V. Menon, A.M. Al-Azawi, H. Tarazi, H.H. M. Abdu-Allah, A.N. El-Shorbagi, R. El-Awady, Inhibition of SHP2 by new compounds induces differential effects on RAS/RAF/ERK and PI3K/AKT pathways in different cancer cell types, Invest. New Drugs 37 (2019) 252–261.
[20] H.H.M. Abdu-Allah, S.G. Abdel-Moty, R. El-Awady, A.N. El-Shorbagi, Design and synthesis of novel 5-aminosalicylate (5-ASA)-4-thiazolinone hybrid derivatives with promising antiproliferative activity, Bioorg. Med. Chem. Lett. 26 (2016) 1647–1650.
[21] T. Onoda, H. Iinuma, Y. Sasaki, M. Hamada, K. Isshiki, H. Naganawa, T. Takeuchi, K. Tatsuta, K. Umezawa, Isolation of a novel tyrosine kinase inhibitor, lavendustin A, from Streptomyces griseolavendus, J. Nat. Prod. 52 (1989) 1252–11127.
[22] H. Chen, J. Boiziau, F. Parker, R. Maroun, B. Tocque, B.P. Roques, C. Garbay-Jaureguiberry, Synthesis and structure-activity studies of a series of [(hydroxybenzyl) amino] salicylates as inhibitors of EGF receptor-associated tyrosine kinase activity, J. Med. Chem. 36 (1993) 4094–4408.
[23] T. Onoda, K. Isshiki, T. Takeuchi, K. Tatsuta, K. Umezawa, Inhibition of tyrosine kinase and epidermal growth factor receptor internalization by lavendustin A methyl ester in cultured A431 cells, Drugs. Exp. Clin. Res. 16 (1990) 249–253.
[24] P. Nussbaumer, A.P. Winiski, S. Cammisuli, P. Hiestand, G. Weckbecker, A. Stuetz, Novel antiproliferative agents derived from lavendustin A, J. Med. Chem. 37 (1994) 4079–4084.
[25] H. Chen, J. Boiziau, F. Parker, P. Mailliet, A. Commercon, B. Tocque, J.-B. Le Pecq, B.-P. Roques, C. Garbay, Structure-activity relationships in a series of 5-[(2, 5-dihydroxybenzyl) amino] salicylate inhibitors of EGF-receptor-associated tyrosine kinase: importance of additional hydrophobic aromatic interactions, J. Med. Chem. 37 (1994) 845–859.
[26] T. Liu, R. Shirai, T. Matsui, K. Umezawa, S. Iwasaki, Synthesis and biological activity of 5-[(2,5-dihydroxybenzyl)amino]salicylic acid analogs as inhibitors of

EGF receptor-associated protein tyrosine kinase, Bioorg. Med. Chem. Lett. 7 (1997) 365–1338.
[27] F. Mu, S.L. Coffing, D.J. Riese, R.L. Geahlen, P. Verdier-Pinard, E. Hamel, J. Johnson, M. Cushman, Design, synthesis, and biological evaluation of a series of lavendustin A analogues that inhibit EGFR and Syk tyrosine kinases, as well as tubulin polymerization, J. Med. Chem. 44 (2001) 441–452.
[28] D. Song, Y. Park, J. Yoon, W. Aman, J.-M. Hah, J.-S. Ryu, Click approach to the discovery of 1, 2, 3-triazolylsalicylamides as potent Aurora kinase inhibitors, Bioorg. Med. Chem. 22 (2014) 4855–4866.
[29] L.L. de Carvalho, R. Bittencourt Pena, N. Correia Romeiro, J.L. Nepomuceno-Silva, A concise synthesis of triazole analogues of lavendustin A via click chemistry approach and preliminary evaluation of their antiparasitic activity against Trypanosoma cruzi, Chem. Select. 7 (2022) e202200128.
[30] W.K. Agbotounou, K. Umezawa, A. Jacquemin-Sablon, J. Pierre, Inhibition by two lavendustins of the tyrosine kinase activity of pp60F527 in vitro and in intact cells, Eur. J. Pharmacol. 269 (1994) 1–8.
[31] M.K. El-Nagar, H.H.M. Abdu-Allah, O.I. Salem, A.-H.-N. Kafafy, H.S. Farghaly, Novel N-substituted 5-aminosalicylamides as dual inhibitors of cyclooxygenase and 5-lipoxygenase enzymes: synthesis, biological evaluation and docking study, Bioorg. Chem. 78 (2018) 80–93.
[32] S. Ramos-Inza, A.C. Ruberte, C. Sanmartín, A.K. Sharma, D. Plano, NSAIDs: old acquaintance in the pipeline for cancer treatment and prevention–structural modulation, mechanisms of action, and bright future, J. Med. Chem. 64 (2021) 16380–16421.
[33] L.J. Marnett, Inflammation and cancer: chemical approaches to mechanisms, imaging, and treatment, J. Org. Chem. 77 (2012) 5224–5238.
[34] A. Aliabadi, E. Khanniri, M. Mahboubi-Rabbani, M. Bayanati, Dual COX-2/15-LOX inhibitors: a new avenue in the prevention of cancer, Eur. J. Med. Chem. 261 (2023) 115866.
[35] C. Bathula, S. Tripathi, R. Srinivasan, K.K. Jha, A. Ganguli, G. Chakrabarti, S. Singh, P. Munshi, S. Sen, Synthesis of novel 5-arylidenethiazolidinones with apoptotic properties via a three component reaction using piperidine as a bifunctional reagent, Org. Biomol. Chem. 14 (2016) 8053–8063.
[36] D. Havrylyuk, B. Zimenkovsky, O. Vasylenko, L. Zaprutko, A. Gzella, R. Lesyk, Synthesis of novel thiazolone-based compounds containing pyrazoline moiety and evaluation of their anticancer activity, Eur. J. Med. Chem. 44 (2009) 1396–1404.
[37] C. Boureghda, R. Boulcina, V. Dorcet, F. Berrée, B. Carboni, A. Debache, Facile synthesis of 5-arylidene rhodanine derivatives using Na2SO3 as an eco-friendly catalyst. Access to 2-mercapto-3-aryl-acrylic acids and a benzoxaborole derivative, Tetrahedron Lett. 62 (2021) 152690.
[38] E. Campaigne, R.E. Cline, Preparation and absorption spectra of some β-aryl-α-mercaptoacrylic acids and related disulfides 1,2, J. Org. Chem. 21 (1956) 32–38.
[39] E. Brun, A. Safer, F. Carreaux, K. Bourahla, M. L'Helgoua'ch, J.P. Bazureau, J. M. Villalgordo, Microwave-assisted condensation reactions of acetophenone derivatives and activated methylene compounds with aldehydes catalyzed by boric acid under solvent-free conditions, Molecules 20 (2015) 11617–11631.
[40] S.D. Bull, S.G. Davies, G. Fenton, A.W. Mulvaney, R.S. Prasad, A.D. Smith, Chemoselective debenzylation of *N*-benzyl tertiary amines with ceric ammonium nitrate, J. Chem. Soc. Perkin Trans. 1 (2000) 3765–3774.
[41] J. Bhaskar Kanth, C.K. Reddy, M. Periasamy, Convenient method for *N*-debenzylation of tertiary amines, Synth. Commun. 24 (1994) 313–339.
[42] P. Wee, Z. Wang, Epidermal growth factor receptor cell proliferation signaling pathways, Cancers 9 (2017) 52.
[43] N.A.E.A. Kassab, Indian J. Chem. - B Org. Med. 14 (1976) 864–887.
[44] R.A. El-Awady, E.M. Saleh, M. Ezz, A.M. Elsayed, Interaction of celecoxib with different anti-cancer drugs is antagonistic in breast but not in other cancer cells, Toxicol. Appl. Pharmacol. 255 (2011) 271–286.
[45] J.L. Nakamura, The epidermal growth factor receptor in malignant gliomas: pathogenesis and therapeutic implications, Expert. Opin. Ther. Targets 11 (2007) 463–472.
[46] A.S. Alanazi, T.O. Mirgany, A.A. Alsfouk, N.A. Alsaif, M.M. Alanazi, Antiproliferative activity, multikinase inhibition, apoptosis-inducing effects and molecular docking of novel isatin-purine hybrids, Medicina 59 (2023) 610.
[47] R.M. Mohareb, N.M.A. Bagato, I.T. Radwan, Design, synthesis, molecular docking, and biological studies of new heterocyclic compounds derived from β-diketones as novel EGFR and Pim-1 inhibitors endowed with antitumor activity, Curr. Med. Chem. Anticancer Agents 22 (2022) 2558–2576.